fractal and fractional

Article

New Method to Investigate the Impact of Independent Quadratic α-Stable Poisson Jumps on the Dynamics of a Disease under Vaccination Strategy

Yassine Sabbar [1], Asad Khan [2,*], Anwarud Din [3,*] and Mouhcine Tilioua [1]

[1] MAIS Laboratory, MAMCS Group, FST Errachidia, Moulay Ismail University of Meknes, P.O. Box 509, Errachidia 52000, Morocco
[2] School of Computer Science and Cyber Engineering, Guangzhou University, Guangzhou 510006, China
[3] Department of Mathematics, Sun Yat-sen University, Guangzhou 510006, China
[*] Correspondence: asad@gzhu.edu.cn (A.K.); anwarud@mail.sysu.edu.cn (A.D.)

Abstract: Long-run bifurcation analysis aims to describe the asymptotic behavior of a dynamical system. One of the main objectives of mathematical epidemiology is to determine the acute threshold between an infection's persistence and its elimination. In this study, we use a more comprehensive SVIR epidemic model with large jumps to tackle this and related challenging problems in epidemiology. The huge discontinuities arising from the complexity of the problem are modelled by four independent, tempered, α-stable quadratic Lévy processes. A new analytical method is used and for the proposed stochastic model, the critical value $\mathfrak{R}_0^\star$ is calculated. For strictly positive value of $\mathfrak{R}_0^\star$, the stationary and ergodic properties of the perturbed model are verified (continuation scenario). However, for a strictly negative value of $\mathfrak{R}_0^\star$, the model predicts that the infection will vanish exponentially (disappearance scenario). The current study incorporates a large number of earlier works and provides a novel analytical method that can successfully handle numerous stochastic models. This innovative approach can successfully handle a variety of stochastic models in a wide range of applications. For the tempered α-stable processes, the Rosinski (2007) algorithm with a specific Lévy measure is implemented as a numerical application. It is concluded that both noise intensities and parameter α have a great influence on the dynamical transition of the model as well as on the shape of its associated probability density function.

Keywords: dynamical system; noise; bifurcation; ergodicity; lévy processes; jumps

MSC: 37A30; 34H20; 34E10; 34D10

check for updates

Citation: Sabbar, Y.; Khan, A.; Din, A.; Tilioua, M. New Method to Investigate the Impact of Independent Quadratic α-Stable Poisson Jumps on the Dynamics of a Disease under Vaccination Strategy. *Fractal Fract.* **2023**, *7*, 226. https://doi.org/10.3390/fractalfract7030226

Academic Editors: Xin-Guang Yang, Baowei Feng and Xingjie Yan

Received: 28 December 2022
Revised: 11 February 2023
Accepted: 27 February 2023
Published: 2 March 2023

1. Introduction

For the last two centuries, infectious diseases have been identified as the greatest impediment to human civilization. These infectious illnesses (particularly the emerging epidemics) have caused a huge number of health and economic problems [1], and thus, investigating the dynamics and control of such diseases is the focal point of today's researchers. For instance, the pandemic COVID-19 has very serious consequences (for health, economy, culture, education, etc.), with more than 200 million confirmed cases worldwide, including more than 4 million deaths [2]. Human influenza, a contagious respiratory infection caused by influenza viruses, has a seasonal pattern and, to date, is assumed to be a major public health problem. In *Morocco*, it affects about 1 to 5 million people each year and causing between 17,000 and 30,000 deaths [2]. The Ebola virus illness produced a large outbreak in *West Africa* in 2016, with at least 28,600 officially recognized cases and over 11,325 deaths [2]. In this situation, developing tools to better understand the dynamics driving the epidemic's spread is critical for guiding public health strategies [3]. Developing a mechanistic model that drives the dynamics of such diseases and contains the criteria that characterise them is a natural way to describe their prevalence [4]. Nonetheless, due to the unique way infectious diseases spread, the finding of a straightforward technique that precisely predicts their behavior is highly desired [5]. In that respect, mathematical biology, notably through compartmental formulations, is considered the most substantial means to depict the epidemiological dynamics of pathogen transmission. Furthermore, the subject research may aid policymakers and health officials in developing and implementing an effective control strategy to reduce the spread of an infectious disease [6]. Besides other control interventions, vaccination is assumed to be the most effective strategy for restricting the spread of *COVID-19* [7]. Many countries have approved vaccines for emergency use from *Pfizer/BioNTech*, *Janssen*, *Sinopharm*, *Astra-Zeneca*, and *Sputnik V* [2]. As of 23 April 2022, the health department reported that 24,898,497 people had been vaccinated in *Morocco*, providing significant group immunity against this virus. Consequently, the epidemiological condition began to improve, with the goal of completely eliminating the disease. We focus on an infection model with four groups in this study by considering the vaccination strategy's application (see Table 1).

Table 1. A list of the different groups of the studied population.

Group	Biological Classification
$\mathbf{G}_1$	Sensitive people
$\mathbf{G}_2$	Vaccinated people
$\mathbf{G}_3$	Infected people
$\mathbf{G}_4$	Recovered people with total immunity

The movements between these groups are characterized by the following deterministic system:

$$\begin{cases} \mathrm{d}\mathbf{G}_1(t) = \Bigg(\overbrace{\mathfrak{r}\mathbf{G}_1(t)\left(1 - \frac{\mathbf{G}_1(t)}{\mathcal{K}}\right)}^{\text{Logistic growth}} - \beta_1 \overbrace{\mathcal{H}_1\big(\mathbf{G}_1(t), \mathbf{G}_3(t)\big)}^{\text{Functional response}} \mathbf{G}_3(t) - (\mathfrak{u} + \varpi)\mathbf{G}_1(t)\Bigg)\mathrm{d}t, \\ \mathrm{d}\mathbf{G}_2(t) = \Big(\varpi\mathbf{G}_1(t) - \beta_2\mathcal{H}_2(\mathbf{G}_2(t), \mathbf{G}_3(t))\mathbf{G}_3(t) - (\mathfrak{u} + \varsigma)\mathbf{G}_2(t)\Big)\mathrm{d}t, \\ \mathrm{d}\mathbf{G}_3(t) = \Big(\beta_1\mathcal{H}_1(\mathbf{G}_1(t), \mathbf{G}_3(t))\mathbf{G}_3(t) + \beta_2\mathcal{H}_2(\mathbf{G}_2(t), \mathbf{G}_3(t))\mathbf{G}_3(t) - (\mathfrak{u} + \mathfrak{a} + \mathfrak{c})\mathbf{G}_3(t)\Big)\mathrm{d}t, \\ \mathrm{d}\mathbf{G}_4(t) = \Big(\varsigma\mathbf{G}_2(t) + \mathfrak{c}\mathbf{G}_3(t) - \mathfrak{u}\mathbf{G}_4(t)\Big)\mathrm{d}t, \end{cases} \tag{1}$$

where, $\mathfrak{r}$ designates the inherent growth rate of $\mathbf{G}_1$, $\mathcal{K}$ is the standard carrying capacity of the environment, ϖ is the vaccination rate, β_1 is the transmission coefficient between $\mathbf{G}_1$ and $\mathbf{G}_3$, β_2 indicates the infection transmission rate between $\mathbf{G}_2$ and $\mathbf{G}_3$ before obtaining the immunity, ς is the recovery rate of $\mathbf{G}_2$, $\mathfrak{u}$ and $\mathfrak{a}$ are respectively the natural and the infection-induced death rates, lastly, $\mathfrak{c}$ is the recovery rate of $\mathbf{G}_3$. Due to some analytical reasons, we assume that $\eta^{\star\star} = \mathfrak{r} - (\mathfrak{u} + \varpi)$ is positive. The functions $\mathcal{H}_1(\mathbf{G}_1, \mathbf{G}_3)$ and $\mathcal{H}_2(\mathbf{G}_2, \mathbf{G}_3)$ appearing in system (1) denote the general incidence rates and biologically, these functions shows the number of cases being infected in a unit time. These two interference functions characterize the cross-infections, and their forms include the vast majority of response examples found in the literature. For ease of reading, in the remaining parts of this manuscript, we outline the transmission mechanisms of the above-mentioned model by the flow diagram shown in Figure 1. Analytically, we suppose that the general interference responses $\mathcal{H}_1, \mathcal{H}_2 \in C^2(\mathbb{R}_+ \times \mathbb{R}_+, \mathbb{R}_+)$ and satisfies the following two conditions:

- $\mathbf{C}_\mathbf{a}$: $\mathcal{H}_1(0, \mathbf{G}_3) = 0$, $\mathcal{H}_2(0, \mathbf{G}_3) = 0$ $\forall \mathbf{G}_3 \geq 0$; $\mathcal{H}_1$ is increasing in $\mathbf{G}_1$ and decreasing in $\mathbf{G}_3$; $\mathcal{H}_2$ is increasing in $\mathbf{G}_2$ and decreasing in $\mathbf{G}_3$; and there exists two positive constants Δ_1, Δ_2 such that

$$\frac{\partial\mathcal{H}_1(\mathbf{G}_1, \mathbf{G}_3)}{\partial\mathbf{G}_1} \leq \Delta_1, \qquad \frac{\partial\mathcal{H}_2(\mathbf{G}_2, \mathbf{G}_3)}{\partial\mathbf{G}_2} \leq \Delta_2,$$

for all $\mathbf{G}_1, \mathbf{G}_2, \mathbf{G}_3 \geq 0$.

- $\mathbf{C_b}$: $\mathcal{H}_1$ and $\mathcal{H}_2$ follow the uniform continuity property at $\mathbf{G}_3 = 0$:

$$\begin{cases} \lim\limits_{\mathbf{G}_3 \to 0} \sup\limits_{\mathbf{G}_1 > 0} \{|\mathcal{H}_1(\mathbf{G}_1, \mathbf{G}_3) - \mathcal{H}_1(\mathbf{G}_1, 0)|\} = 0, \\ \lim\limits_{\mathbf{G}_3 \to 0} \sup\limits_{\mathbf{G}_2 > 0} \{|\mathcal{H}_2(\mathbf{G}_2, \mathbf{G}_3) - \mathcal{H}_2(\mathbf{G}_2, 0)|\} = 0. \end{cases}$$

The above properties are readily satisfied by the typical examples listed in Tables 2 and 3.

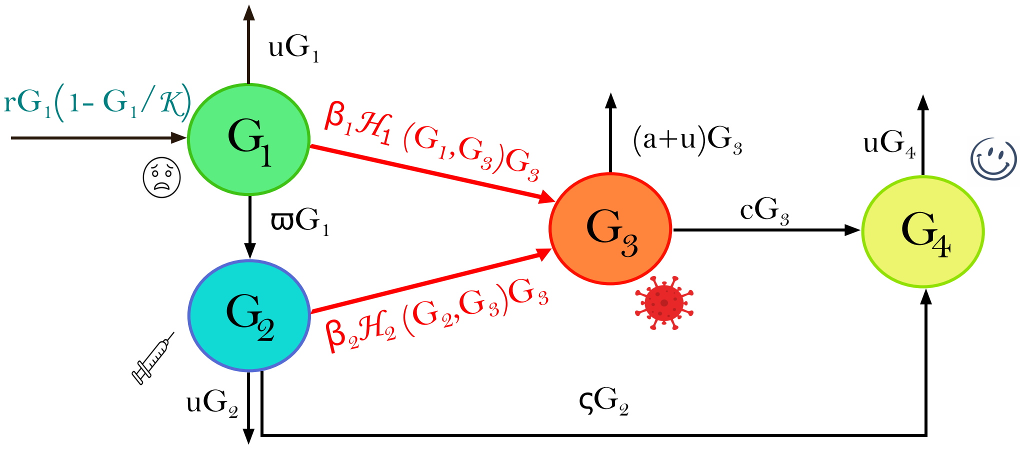

Figure 1. The diagram of the deterministic epidemic model (1). Different transfer rates between the classes are illustrated by arrows.

Table 2. List of some prototypes of the general interference function $\mathcal{H}_1$.

Name	Expression
Bilinear	$\mathcal{H}_1(\mathbf{G}_1, \mathbf{G}_3) = \mathbf{G}_1$
Saturated 2	$\mathcal{H}_1(\mathbf{G}_1, \mathbf{G}_3) = \dfrac{\mathbf{G}_1}{\mathfrak{q} + \mathbf{G}_1}, (\mathfrak{q} > 0)$
Dual saturated	$\mathcal{H}_1(\mathbf{G}_1, \mathbf{G}_3) = \dfrac{\mathbf{G}_1^2}{(\mathfrak{q}_1 + \mathbf{G}_1)(\mathfrak{q}_2 + \mathbf{G}_1)}, (\mathfrak{q}_1, \mathfrak{q}_2 > 0)$
Beddington-DeAngelis	$\mathcal{H}_1(\mathbf{G}_1, \mathbf{G}_3) = \dfrac{\mathbf{G}_1}{1 + \mathfrak{q}_1\mathbf{G}_1 + \mathfrak{q}_2\mathbf{G}_3}, (\mathfrak{q}_1, \mathfrak{q}_2 > 0)$
Crowley-Martin	$\mathcal{H}_1(\mathbf{G}_1, \mathbf{G}_3) = \dfrac{\mathbf{G}_1}{(\mathfrak{q}_1 + \mathbf{G}_1)(\mathfrak{q}_2 + \mathbf{G}_3)}, (\mathfrak{q}_1, \mathfrak{q}_2 > 0)$
Modified Crowley-Martin	$\mathcal{H}_1(\mathbf{G}_1, \mathbf{G}_3) = \dfrac{\mathbf{G}_1}{1 + \mathfrak{q}_1\mathbf{G}_1 + \mathfrak{q}_2\mathbf{G}_3 + \mathfrak{q}_3\mathbf{G}_1\mathbf{G}_3}, (\mathfrak{q}_1, \mathfrak{q}_2, \mathfrak{q}_3 > 0)$

In [8], the authors treated the epidemic model (1) in its particular case with functional response type 1. They proved that the deterministic critical value is expressible in the form of:

$$\mathfrak{R}_\circ = \frac{\beta_1 \mathcal{K}\eta^{\star\star}(\mathfrak{u} + \varsigma) + \beta_2 \mathcal{K}\varpi\eta^{\star\star}}{\mathfrak{r}(\mathfrak{u} + \varsigma)(\mathfrak{u} + \mathfrak{a} + \mathfrak{c})} = \frac{1}{(\mathfrak{u} + \mathfrak{a} + \mathfrak{c})}\left(\beta_1 \overbrace{\frac{\mathcal{K}\eta^{\star\star}}{\mathfrak{r}}}^{=\mathbf{G}_1^\circ} + \beta_2 \overbrace{\frac{\mathcal{K}\eta^{\star\star}\varpi}{\mathfrak{r}(\mathfrak{u} + \varsigma)}}^{=\mathbf{G}_2^\circ}\right).$$

This quantity allows us to classify the dynamics of infection and predict its long-run behavior. That is, if $\mathfrak{R}_\circ < 1$, then the infection will disappear, while the endemic nature of the infection occurs for $\mathfrak{R}_\circ > 1$.

Table 3. List of some prototypes of the general interference function $\mathcal{H}_2$.

Name	Expression
Bilinear	$\mathcal{H}_2(\mathbf{G}_2, \mathbf{G}_3) = \mathbf{G}_2$
Saturated	$\mathcal{H}_2(\mathbf{G}_2, \mathbf{G}_3) = \dfrac{\mathbf{G}_2}{\mathfrak{q}^\star + \mathbf{G}_2}, (\mathfrak{q}^\star > 0)$
Dual saturated	$\mathcal{H}_2(\mathbf{G}_2, \mathbf{G}_3) = \dfrac{\mathbf{G}_2^2}{(\mathfrak{q}_1^\star + \mathbf{G}_2)(\mathfrak{q}_2^\star + \mathbf{G}_2)}, (\mathfrak{q}_1^\star, \mathfrak{q}_2^\star > 0)$
Beddington-DeAngelis	$\mathcal{H}_2(\mathbf{G}_2, \mathbf{G}_3) = \dfrac{\mathbf{G}_2}{1 + \mathfrak{q}_1^\star \mathbf{G}_2 + \mathfrak{q}_2^\star \mathbf{G}_3}, (\mathfrak{q}_1^\star, \mathfrak{q}_2^\star > 0)$
Crowley-Martin	$\mathcal{H}_2(\mathbf{G}_2, \mathbf{G}_3) = \dfrac{\mathbf{G}_2}{(\mathfrak{q}_1^\star + \mathbf{G}_2)(\mathfrak{q}_2^\star + \mathbf{G}_3)}, (\mathfrak{q}_1^\star, \mathfrak{q}_2^\star > 0)$
Modified Crowley-Martin	$\mathcal{H}_2(\mathbf{G}_2, \mathbf{G}_3) = \dfrac{\mathbf{G}_2}{1 + \mathfrak{q}_1^\star \mathbf{G}_2 + \mathfrak{q}_2^\star \mathbf{G}_3 + \mathfrak{q}_3^\star \mathbf{G}_2 \mathbf{G}_3}, (\mathfrak{q}_1^\star, \mathfrak{q}_2^\star, \mathfrak{q}_3^\star > 0)$

In reality, external variations affect the spread of an infection and make it more tricky to predict its behavior [9]. Epidemic systems are totally sophisticated and complex. One of the characteristics of complexity is the randomness and uncertainties, either in the reasons for a phenomenon that has occurred, or in the prediction of its long-term evolution [10]. The stochastic approach highlights many assumptions and concerns when studying the dynamics of a system. For this reason, multiplicative and additive noise sources carry out a significant role in the transient dynamics of biological and physical systems [11]. Technically, if the noise level is abnormally high, the signal can be drowned out, similar logic for biological systems where noises help in reducing the infection [12]. Regarding the physical understanding of biological models, the above two types of casual noise have been widely used. Patently, additive noise is characterized by its proactive role in the transient dynamics of dynamical systems, and multiplicative noise is responsible for noise-induced transitions [13]. In such situations, deterministic formulations, which are able to make very instructive predictions and forecasts, are not close enough to reality to warrant reliance [14–17]. Consequently, we need an improved and sophisticated mathematical framework that takes into consideration the randomness effect, especially when studying the prevalence of a highly harmful infectious disease like COVID-19 [18]. In this regard, plenty of researchers have proposed and developed a variety of perturbed models that simulate the dynamics of a number of diseases from different perspectives [19–25]. In all these surveys, the transit from the deterministic setting to the probabilistic one is done by presuming that the parameter values fluctuate around their value in a natural way, which is often expressed by perturbing the system with white noises. The introduction of these fluctuations is considered to be one of the most logical and eminent ways of depicting any real phenomenon under slight and continuous oscillations. Regrettably, concept is lacking in describing the spread of infection during large and unexpected environmental disturbances, during economic crises, or through the use of human interventions (vaccination strategy in the case of COVID-19 [7]). For this ground, we looking to the use of Lévy processes which are famous for their capability to decently formulate this sort of stochasticity. This formulation can be upgraded by using the the quadratic Lévy noise to model the complexity of certain physical impulses caused by massive extrinsic disturbances [26–28]. In addition, the standard Lévy formulation is based on distributions which have partially-weighty tails, and consequently they have limited potential to simulate radical and brutal phenomena which usually lead to unexpected variations in the total number of individuals [27–35].

Stable Lévy distributions were originally introduced for financial returns by Mandelbrot in 1963 [36]. They offer an advantage over the log-normal assumption in that extreme and great events can exist in the model. They have not been widely used due to the difficulty of performing the calculations [37]. Most models using stable distributions also assume that they are stationary; when the parameters are fitted to a stationary stable model, the tails turn out to be systematically too heavy. A α-stable Lévy process can be represented as a combination of a (compound) Poisson process and a Brownian motion. For small values of α, we see that the process is dominated by big jumps. For medium values (e.g., $\alpha = 1$, i.e., Cauchy process) we get both small and large jumps. For α close to 2, we get Brownian motion with occasional jumps (see Figure 2). α-stable processes for $\alpha \in (0, 2)$ have infinite variance, which makes them somewhat inconvenient. Nevertheless, they are important in physics, biology, meteorology, and have been used in option pricing in finance [38–40].

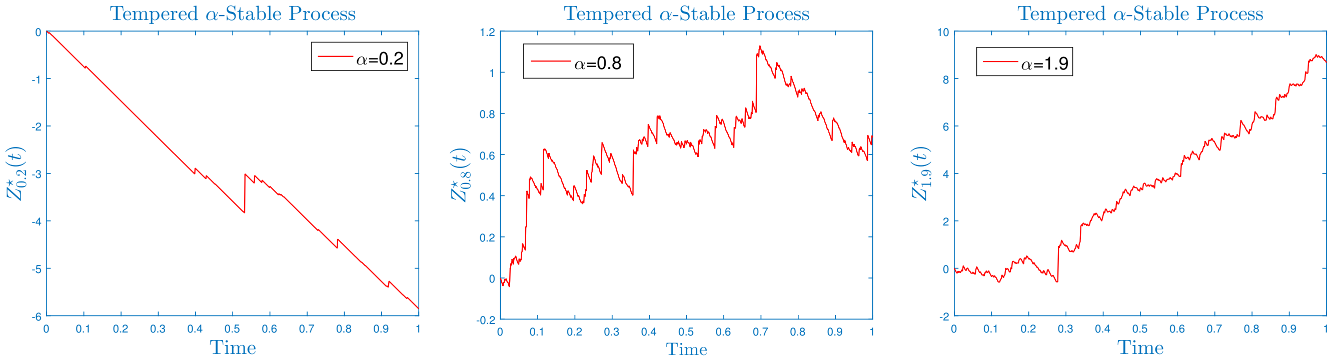

Figure 2. Numerical illustration of sample paths of the single-sided tempered α-stable process $\mathbb{Y}(t)$ when $\alpha = 0.2, 0.8, 1.2$ and 1.9. The inputs tuning of the used algorithm are as follows: $\varsigma_{\star,-} = 0$, $\varsigma_{\star,+} = 2.8$, $\kappa_{\star,-} = 1.2$ and $\kappa_{\star,+} = 1.2$.

In many epidemiological models, the largest jumps are frequently ignored. Lévy's tempered motion adopts a different approach, exponentially tempering the probability of massive jumps, so that remarkably large jumps are extremely unlikely and all moments exist [41]. Tempering stable processes offer technical advantages, since the jumps process remains an infinitely divisible Lévy process whose governing equation can be identified and whose transition densities can be calculated at any scale [42]. These transition densities solve a tempered fractional diffusion equation, quite similar to the fractional diffusion equation. Like the truncated Lévy flights, they evolve from an early super-diffusive behavior to a late diffusive behavior of the disease.

In this research, we investigate the impact of tempered α-stable Lévy distribution on the dynamics of an epidemiological model. This scope is new and puts forward a novel analytical approach that deals with epidemic models under heavy variations. Inspired by the above facts and motivations, the improved version of system (1) will take the following shape:

$$\begin{cases} \mathrm{d}\mathbf{G}_1(t) = \overbrace{\left(\mathfrak{r}\mathbf{G}_1(t)\left(1 - \dfrac{\mathbf{G}_1(t)}{\mathcal{K}}\right) - \beta_1 \mathcal{H}_1(\mathbf{G}_1(t), \mathbf{G}_3(t))\mathbf{G}_3(t) - (\mathfrak{u} + \varpi)\mathbf{G}_1(t)\right)}^{\text{Deterministic part}} \mathrm{d}t + \overbrace{\mathrm{d}\mathbf{S}_1(t)}^{\text{Fluctuations}}, \\ \mathrm{d}\mathbf{G}_2(t) = \left(\varpi\mathbf{G}_1(t) - \beta_2\mathcal{H}_2(\mathbf{G}_2(t), \mathbf{G}_3(t))\mathbf{G}_3(t) - (\mathfrak{u} + \varsigma)\mathbf{G}_2(t)\right)\mathrm{d}t + \mathrm{d}\mathbf{S}_2(t), \\ \mathrm{d}\mathbf{G}_3(t) = \left(\beta_1\mathcal{H}_1(\mathbf{G}_1(t), \mathbf{G}_3(t))\mathbf{G}_3(t) + \beta_2\mathcal{H}_2(\mathbf{G}_2(t), \mathbf{G}_3(t))\mathbf{G}_3(t) - (\mathfrak{u} + \mathfrak{a} + \mathfrak{c})\mathbf{G}_3(t)\right)\mathrm{d}t + \mathrm{d}\mathbf{S}_3(t), \\ \mathrm{d}\mathbf{G}_4(t) = \left(\varsigma\mathbf{G}_2(t) + \mathfrak{c}\mathbf{G}_3(t) - \mathfrak{u}\mathbf{G}_4(t)\right)\mathrm{d}t + \mathrm{d}\mathbf{S}_4(t), \end{cases} \quad (2)$$

where

$$\begin{cases} \mathrm{d}\mathbf{S}_1(t) & = \overbrace{\big(\zeta_{1L}\mathbf{G}_1(t) + \zeta_{1Q}\mathbf{G}_1^2(t)\big)\mathrm{d}\mathcal{B}_1(t)}^{\text{Quadratic white noise}} + \overbrace{\int_\chi \big(\theta_{1L}(u)\mathbf{G}_1(t^-) + \theta_{1Q}(u)\mathbf{G}_1^2(t^-)\big)\widetilde{\mathcal{C}}_1^\alpha(\mathrm{d}t, \mathrm{d}u)}^{\text{Quadratic tempered stable jumps}}, \\ \mathrm{d}\mathbf{S}_2(t) & = \big(\zeta_{2L}\mathbf{G}_2(t) + \zeta_{2Q}\mathbf{G}_2^2(t)\big)\mathrm{d}\mathcal{B}_2(t) + \int_\chi \big(\theta_{2L}(u)\mathbf{G}_2(t^-) + \theta_{2Q}(u)\mathbf{G}_2^2(t^-)\big)\widetilde{\mathcal{C}}_2^\alpha(\mathrm{d}t, \mathrm{d}u), \\ \mathrm{d}\mathbf{S}_3(t) & = \big(\zeta_{3L}\mathbf{G}_3(t) + \zeta_{3Q}\mathbf{G}_3^2(t)\big)\mathrm{d}\mathcal{B}_3(t) + \int_\chi \big(\theta_{3L}(u)\mathbf{G}_3(t^-) + \theta_{3Q}(u)\mathbf{G}_3^2(t^-)\big)\widetilde{\mathcal{C}}_3^\alpha(\mathrm{d}t, \mathrm{d}u), \\ \mathrm{d}\mathbf{S}_4(t) & = \big(\zeta_{4L}\mathbf{G}_4(t) + \zeta_{4Q}\mathbf{G}_4^2(t)\big)\mathrm{d}\mathcal{B}_4(t) + \int_\chi \big(\theta_{4L}(u)\mathbf{G}_4(t^-) + \theta_{4Q}(u)\mathbf{G}_4^2(t^-)\big)\widetilde{\mathcal{C}}_4^\alpha(\mathrm{d}t, \mathrm{d}u). \end{cases}$$

To well characterize the probabilistic part of the updated model, firstly, we define the underlying probability space $(\Omega_\mathcal{E}, \mathcal{E}, \mathbb{P}_\Omega)$ with its associated filtration $\{\mathcal{E}_t\}_{t\geq 0}$ (right continuous, increasing and $\mathcal{E}_0$ encompasses all $\mathbb{P}_\Omega$-null collections). Before moving further, let us explain the notations, processes and measures appearing in system (2):

- $\mathbf{G}_\ell(t^-)$ indicate the left limits of $\mathbf{G}_\ell(t)$ $(\ell = 1, 2, 3, 4)$.
- $\mathcal{B}_\ell(t)$ $(\ell = 1, 2, 3, 4)$ are alternately independent Wiener processes presented on $(\Omega_\mathcal{E}, \mathcal{E}, \{\mathcal{E}_t\}_{t\geq 0}, \mathbb{P}_\Omega)$.
- $\zeta_{\ell L}$ $(\ell = 1, 2, 3, 4)$ denote the linear diffusion amplitudes; and $\zeta_{\ell Q}$ $(\ell = 1, 2, 3, 4)$ represent the strengths of quadratic fluctuations.
- $\widetilde{\mathcal{C}}_\ell^\alpha$ $(\ell = 1, 2, 3, 4)$ are the mutually independent compensator processes associated respectively with the Poisson random measures $\mathfrak{N}_\ell$ $(\ell = 1, 2, 3, 4)$.
- $\mathfrak{N}_\ell$ $(\ell = 1, 2, 3, 4)$ are independent to $\mathcal{B}_\ell$ $(\ell = 1, 2, 3, 4)$.
- $\mathfrak{Z}_\ell^\alpha(\cdot)$ $(\ell = 1, 2, 3, 4)$ are the tempered α-stable Lévy measures defined on a measurable set $\chi \subset (0, \infty)$.
- $\mathfrak{Z}_\ell^\alpha(\chi) < \infty$ $(\ell = 1, 2, 3, 4)$ and $\widetilde{\mathcal{C}}_\ell^\alpha(t, \mathrm{d}u)$ $(\ell = 1, 2, 3, 4)$ are $\{\mathcal{E}_t\}$-martingales, where

$$\begin{cases} \mathfrak{N}_1(t, \mathrm{d}u) = \widetilde{\mathcal{C}}_1^\alpha(t, \mathrm{d}u) + t\mathfrak{Z}_1^\alpha(\mathrm{d}u), \\ \mathfrak{N}_2(t, \mathrm{d}u) = \widetilde{\mathcal{C}}_2^\alpha(t, \mathrm{d}u) + t\mathfrak{Z}_2^\alpha(\mathrm{d}u), \\ \mathfrak{N}_3(t, \mathrm{d}u) = \widetilde{\mathcal{C}}_3^\alpha(t, \mathrm{d}u) + t\mathfrak{Z}_3^\alpha(\mathrm{d}u), \\ \mathfrak{N}_4(t, \mathrm{d}u) = \widetilde{\mathcal{C}}_4^\alpha(t, \mathrm{d}u) + t\mathfrak{Z}_4^\alpha(\mathrm{d}u). \end{cases}$$

- The tempered α-stable Lévy measures $\mathfrak{Z}_\ell^\alpha$ $(\ell = 1, 2, 3, 4)$ are expressed as follows:

$$\mathfrak{Z}_\ell^\alpha(\mathcal{Y}) = \int_{\mathbb{R}_+}\int_\chi e^{-\tau}\tau^{-\alpha-1}\mathbb{1}_\mathcal{Y}(\tau y)\mathfrak{H}_\alpha(\mathrm{d}y)\mathrm{d}\tau, \qquad \alpha \in (0, 2). \tag{3}$$

Here, $\mathfrak{H}_\alpha(\cdot)$ denotes a measure on χ such that $\int_\chi \min\left(\|y\|^2, \|y\|^\alpha\right)\mathfrak{Z}_\alpha(\mathrm{d}y) < \infty$. According to the theory presented in [29], we take

$$\mathfrak{H}_\alpha(\mathrm{d}y) = \phi_-^\star(\mathrm{d}y) + \phi_+^\star(\mathrm{d}y),$$

where

$$\begin{cases} \phi_-^\star = \varsigma_{\star,-}\kappa_{\star,-}^\alpha\delta_{(-1/\kappa_{\star,-}, -1/\kappa_{\star,-}, -1/\kappa_{\star,-}, -1/\kappa_{\star,-})}, \\ \phi_+^\star = \varsigma_{\star,+}\kappa_{\star,+}^\alpha\delta_{(1/\kappa_{\star,+}, 1/\kappa_{\star,+}, 1/\kappa_{\star,+}, 1/\kappa_{\star,+})}, \end{cases}$$

for all $\varsigma_{\star,-}, \varsigma_{\star,+} \geq 0$, $\kappa_{\star,-}, \kappa_{\star,+} > 0$ and δ_z is the Dirac mass measure at point z in $\mathbb{R}^4$. From (3), we infer that the measure $\mathfrak{Z}_i^\alpha$ $(i = 1, 2, 3, 4)$ are rewritten as follows:

$$\mathfrak{Z}_\ell^\alpha(\mathcal{Y}) = \int_{\mathbb{R}_+} \psi_-^\star e^{-\tau}\tau^{-\alpha-1}\mathrm{d}\tau + \int_{\mathbb{R}_+} \psi_+^\star e^{-\tau}\tau^{-\alpha-1}\mathrm{d}\tau, \qquad \alpha \in (0, 2), \tag{4}$$

where

$$\begin{cases} \psi_-^\star = \varsigma_{\star,-}\mathbb{1}_{\mathcal{Y}}(-\tau/\kappa_{\star,-}, -\tau/\kappa_{\star,-}, -\tau/\kappa_{\star,-}, -\tau/\kappa_{\star,-}), \\ \psi_+^\star = \varsigma_{\star,+}\mathbb{1}_{\mathcal{Y}}(\tau/\kappa_{\star,+}, \tau/\kappa_{\star,+}, \tau/\kappa_{\star,+}, \tau/\kappa_{\star,+}). \end{cases}$$

- We principally presume that the intensities $\theta_{\ell L}(u)$ and $\theta_{\ell Q}(u)$ $(\ell = 1,2,3,4)$ are positive continuous functions that meet the following primary criterion:
  $\mathbf{C_c}$:

$$\begin{cases} \int_{\chi} \theta_{\ell L}^2(u)\mathfrak{Z}_\ell^\alpha(\mathrm{d}u) < \infty, & \ell = 1,2,3,4, \\ \int_{\chi} \theta_{\ell Q}^2(u)\mathfrak{Z}_\ell^\alpha(\mathrm{d}u) < \infty, & \ell = 1,2,3,4. \end{cases}$$

Analogous to the aforementioned deterministic setup, the chief target of stochastic modeling in epidemiology is to define the decisive value responsible for eradication and insistence of the illness, that is, the long-run bifurcation. Since system (2) is perturbed by a quadratic noise, its analysis is both a complicated and fascinating subject. Many researchers have recently addressed the long-term behaviour of infection models using Brownian motion in higher order representation (*see for example*, [23–25]). To our knowledge, to date, biological models driven by quadratic tempered α-stable jumps have not been investigated due to some analytical complexities. The present research strives to cope with the long-run bifurcation of system (2). Of course, ergodic steady distribution implies the permanence of the epidemic. Technically, the well-known approach to checking ergodicity is the Khasminskii theorem, which provides in most cases insufficient criteria [43,44]. Thus, the pivotal question of this research is: what is the acute threshold (extended deterministic threshold) between the permanence and eradication of the infection? Specifically, the present study suggests a novel method for dealing with biological systems perturbed by quadratic noises. We will also explore the sharp criterion for the ergodic property of our model and the disappearance of illness (6). By using two auxiliary equations with tempered α-stable quadratic noises, we establish the threshold quantity $\mathfrak{R}_0^\star$. In other words, if $\mathfrak{R}_0^\star > 0$, then model (2) has a single steady ergodic distribution, and if $\mathfrak{R}_0^\star$ is strictly negative, then the density of the infected class will disappear.

The remaining parts of this research are ordered in the following arrangement: In Section 2, we start by giving some necessary lemmas and techniques, then we introduce the value $\mathfrak{R}_0^\star$ associated with the stochastic system (2). In Section 3, we treat the dynamical bifurcation by proving that $\mathfrak{R}_0^\star$ is the sharp threshold between stationarity and extinction of the illness. Section 4 numerically validates the mathematical outcomes and explores the effect of tempered α-stable quadratic Lévy noises on the behavior of a general SVIR infection model (2).

2. Some Preliminaries and Required Lemmas

The first question in exploring the dynamics of an epidemic model is whether it admits a unique and positive global solution over time. The following lemma shows these properties and ensures the well-posedness of the proposed probabilistic system (2).

Lemma 1. *Let $\mathbf{C_c}$ holds. Then, the stochastic system (2) is biologically and mathematically well-posed in the sense that it has a single solution $\mathbf{G}(t) = \big(\mathbf{G}_1(t), \mathbf{G}_2(t), \mathbf{G}_3(t), \mathbf{G}_4(t)\big) \in \mathbb{R}_+^{4,\star}$ which is positive and global in time, where*

$$\mathbb{R}_+^{4,\star} = \{(z_1, z_2, z_3, z_4) : \ z_1 > 0, z_2 > 0, z_3 > 0, z_4 > 0\}.$$

To create a link between stationarity and permanence properties, we need the following lemma.

Lemma 2. *There exists a specific constant $\eta^{\dagger} > 0$ such that*

$$\begin{cases} \limsup_{t\to\infty} \mathbb{E}_{\{\Omega,\mathbb{P}\}}\big[\mathbf{G}_1(t)\big] \leq \eta^{\dagger}, \\ \limsup_{t\to\infty} \mathbb{E}_{\{\Omega,\mathbb{P}\}}\big[\mathbf{G}_2(t)\big] \leq \eta^{\dagger}, \\ \limsup_{t\to\infty} \mathbb{E}_{\{\Omega,\mathbb{P}\}}\big[\mathbf{G}_3(t)\big] \leq \eta^{\dagger}, \\ \limsup_{t\to\infty} \mathbb{E}_{\{\Omega,\mathbb{P}\}}\big[\mathbf{G}_4(t)\big] \leq \eta^{\dagger}. \end{cases}$$

The above result can be proven by employing an analytical treatment identical to that of Lemma 2.1 in [45].

Next, we explore some long-run characteristics of the boundary equations associated with model (2) in the case of $\mathbf{G}_3(t) = 0$ (absence of the infection). Because of that reason, we use the following two-block auxiliary system with quadratic Lévy noise:

$$\begin{cases} \begin{cases} \mathrm{d}\mathbf{S}_1(t) = \overbrace{\Big(\mathfrak{r}\mathbf{S}_1(t)\Big(1 - \frac{\mathbf{S}_1(t)}{\mathcal{K}}\Big) - (\mathfrak{u}+\varpi)\mathbf{S}_1(t)\Big)\mathrm{d}t}^{\text{Deterministic part when } \mathbf{G}_3(t)=0} + \overbrace{\mathrm{d}\mathbf{S}_1^{\mathbf{S}}(t)}^{\text{Fluctuations}}, \\ \mathbf{S}_1(0) = \mathbf{G}_1(0) > 0, \end{cases} \\ \begin{cases} \mathrm{d}\mathbf{S}_2(t) = \Big(\varpi\mathbf{S}_1(t) - (\mathfrak{u}+\varsigma)\mathbf{S}_2(t)\Big)\mathrm{d}t + \mathrm{d}\mathbf{S}_2^{\mathbf{S}}(t), \\ \mathbf{S}_2(0) = \mathbf{G}_2(0) > 0, \end{cases} \end{cases} \tag{5}$$

where

$$\begin{cases} \mathrm{d}\mathbf{S}_1^{\mathbf{S}}(t) = (\zeta_{1L}\mathbf{S}_1(t) + \zeta_{1Q}\mathbf{S}_1^2(t))\mathrm{d}\mathcal{B}_1(t) + \int_{\chi}(\theta_{1L}(u)\mathbf{S}_1(t^-) + \theta_{1Q}(u)\mathbf{S}_1^2(t^-))\widetilde{\mathcal{C}}_1^{\alpha}(\mathrm{d}t,\mathrm{d}u), \\ \mathrm{d}\mathbf{S}_2^{\mathbf{S}}(t) = (\zeta_{2L}\mathbf{S}_2(t) + \zeta_{2Q}\mathbf{S}_2^2(t))\mathrm{d}\mathcal{B}_2(t) + \int_{\chi}(\theta_{2L}(u)\mathbf{S}_2(t^-) + \theta_{2Q}(u)\mathbf{S}_2^2(t^-))\widetilde{\mathcal{C}}_2^{\alpha}(\mathrm{d}t,\mathrm{d}u). \end{cases}$$

Lemma 3. *Let $\big(\mathbf{S}_1(t),\mathbf{S}_2(t)\big)$ be two Markov processes that verify the two-block auxiliary system (5). Then, we have the following properties:*

1. *System (5) is well-posed.*
2. *$\mathbf{S}_1(t) \geq \mathbf{G}_1(t)$ a.s. and $\mathbf{S}_2(t) \geq \mathbf{G}_2(t)$ a.s. (stochastic comparison result [46]).*
3. *If $\eta^{\star\star} - 0.5\zeta_{1L}^2 - \int_{\chi}\Big(\theta_{1L}(u) - \ln\big(1+\theta_{1L}(u)\big)\Big)\mathfrak{Z}_1^{\alpha}(\mathrm{d}u) > 0$, then for each process, there exists a single invariant probability measure, named respectively as $\pi^{\mathbf{S}_1}$ and $\pi^{\mathbf{S}_2}$.*
4. *$\mathbf{S}_1$ and $\mathbf{S}_2$ follow the ergodic property.*

The proof of this lemma is almost analogous to that of Lemma 2.2 in [11].

Lemma 4. *Presume that $\eta^{\star\star} - 0.5\zeta_{1L}^2 - \int_{\chi}\Big(\theta_{1L}(u) - \ln\big(1+\theta_{1L}(u)\big)\Big)\mathfrak{Z}_1^{\alpha}(\mathrm{d}u) > 0$. Then, the time averages of $\mathbf{S}_1(t)$ and $\mathbf{S}_2(t)$ are estimated as follows:*

$$\begin{cases} \lim_{t\to\infty}\frac{1}{t}\int_0^t \mathbf{S}_1(s)\mathrm{d}s \leq \frac{\mathcal{K}}{(\mathfrak{r}+\mathcal{K}\zeta_{1L}\zeta_{1Q})}\Big\{\eta^{\star\star} - 0.5\zeta_{1L}^2 - \int_{\chi}\Big(\theta_{1L}(u) - \ln\big(1+\theta_{1L}(u)\big)\Big)\mathfrak{Z}_1^{\alpha}(\mathrm{d}u)\Big\} = \varphi_1^{\mathbf{S}} > 0, \\ \lim_{t\to\infty}\frac{1}{t}\int_0^t \mathbf{S}_2(s)\mathrm{d}s \leq \frac{\varpi\mathcal{K}}{(\mathfrak{u}+\varsigma)(\mathfrak{r}+\mathcal{K}\zeta_{1L}\zeta_{1Q})}\Big\{\eta^{\star\star} - 0.5\zeta_{1L}^2 - \int_{\chi}\Big(\theta_{1L}(u) - \ln\big(1+\theta_{1L}(u)\big)\Big)\mathfrak{Z}_1^{\alpha}(\mathrm{d}u)\Big\} = \frac{\varpi\varphi_1^{\mathbf{S}}}{(\mathfrak{u}+\varsigma)} > 0. \end{cases}$$

Proof. See Appendix A. □

Remark 1. *Throughout this research, we always assume that* $\eta^{\star\star} - 0.5\zeta_{1L}^2 - \int_{\chi} \Big(\theta_{1L}(u) - \ln\big(1 + \theta_{1L}(u)\big)\Big)\mathfrak{Z}_1^{\alpha}(\mathrm{d}u) > 0$*. By using the properties of functions* $\mathcal{H}_1$*,* $\mathcal{H}_2$ *(especially, the hypothesis* $\mathbf{C_a}$*) and Lemma 4, we deduce that*

$$\begin{cases} \int_{\mathbb{R}_+} \mathcal{H}_1(x,0)\pi^{\mathbf{S}_1}(\mathrm{d}x) \leq \Delta_1 \int_{\mathbb{R}_+} x\pi^{\mathbf{S}_1}(\mathrm{d}x) = \lim_{t\to\infty} \frac{\Delta_1}{t}\int_0^t \mathbf{S}_1(s)\mathrm{d}s < \infty, \\ \int_{\mathbb{R}_+} \mathcal{H}_2(x,0)\pi^{\mathbf{S}_2}(\mathrm{d}x) \leq \Delta_2 \int_{\mathbb{R}_+} x\pi^{\mathbf{S}_2}(\mathrm{d}x) = \lim_{t\to\infty} \frac{\Delta_2}{t}\int_0^t \mathbf{S}_2(s)\mathrm{d}s < \infty. \end{cases}$$

By using Remark 1, we properly introduce the well-defined threshold of the probabilistic system (2) which can be expressed in the following form:

$$\begin{aligned} \mathfrak{R}_0^{\star} = {} & \beta_1 \int_{\mathbb{R}_+} \mathcal{H}_1(x,0)\pi^{\mathbf{S}_1}(\mathrm{d}x) + \beta_2 \int_{\mathbb{R}_+} \mathcal{H}_2(x,0)\pi^{\mathbf{S}_2}(\mathrm{d}x) - (\mathfrak{u} + \mathfrak{a} + \mathfrak{c}) \\ & - 0.5\zeta_{3L}^2 - \int_{\chi} \Big(\theta_{3L}(u) - \ln\big(1 + \theta_{3L}(u)\big)\Big)\mathfrak{Z}_3^{\alpha}(\mathrm{d}u). \end{aligned}$$

Remark 2. *Note that in the case of the functional response type 1, the threshold is*

$$\mathfrak{R}_0^{\star,1} = \beta_1 \int_0^{\infty} x\pi^{\mathbf{S}_1}(\mathrm{d}x) + \beta_2 \int_0^{\infty} x\pi^{\mathbf{S}_2}(\mathrm{d}x) - (\mathfrak{u} + \mathfrak{a} + \mathfrak{c}) - 0.5\zeta_{3L}^2 - \int_{\chi} \Big(\theta_{3L}(u) - \ln\big(1 + \theta_{3L}(u)\big)\Big)\mathfrak{Z}_3^{\alpha}(\mathrm{d}u).$$

Since the expressions of $\pi^{\mathbf{S}_1}$ *and* $\pi^{\mathbf{S}_2}$ *are unknown, Lemma 4 gives the exact value of the threshold which is presented as:*

$$\mathfrak{R}_0^{\star,1} = \beta_1\mathbf{G}_1^{\circ} + \beta_2\mathbf{G}_2^{\circ} - (\mathfrak{u} + \mathfrak{a} + \mathfrak{c}) - 0.5\zeta_{3L}^2 - \int_{\chi} \Big(\theta_{3L}(u) - \ln\big(1 + \theta_{3L}(u)\big)\Big)\mathfrak{Z}_3^{\alpha}(\mathrm{d}u).$$

In the next subsection, we shall show that $\mathfrak{R}_0^{\star}$ is the threshold among the stationarity and the disappearance of the infection.

3. Long-Run Bifurcation of the Stochastic System (2)

3.1. The Stationarity Case

This section demonstrates a novel method for proving the perturbed system's stationarity and, of course, its ergodicity. The following intriguing lemma describes this procedure.

Lemma 5 (*Limited possibilities result*, [47])**.** *Let* $\mathcal{M} \in \mathbb{R}^n$ *be a stochastic process that verifies the Feller property. Then, the ergodicity and stationarity hold or* $\lim_{t\to\infty}\sup_{\hat{\zeta}} \frac{1}{t}\int_0^t \int_{\mathbb{R}^n} \mathbb{P}_{\Omega}(x;s,\mathbb{D})\hat{\zeta}(\mathrm{d}x)\mathrm{d}s = 0$ *for all closed and bounded subset* $\mathbb{D} \subset \mathbb{R}^n$ *and all elementary distributions* $\hat{\zeta}$ *on* $\mathbb{R}^n$*, where* $\mathbb{P}_{\Omega}(x;s,\mathbb{D})$ *is the probability for* $\mathcal{M}$ *in* $\mathbb{D}$ *with* $\mathcal{M}(0) = x \in \mathbb{R}^n$*.*

Remark 3. *Since the fundamental dynamics of the group* $\mathbf{G}_4$ *has no effect on the behavior of the disease, we can omit the fourth equation of* (2) *and we will only deal with the following reduced system:*

$$\begin{cases} \mathrm{d}\mathbf{G}_1(t) = \Big(\mathfrak{r}\mathbf{G}_1(t)\Big(1 - \frac{\mathbf{G}_1(t)}{\mathcal{K}}\Big) - \beta_1\mathcal{H}_1(\mathbf{G}_1(t),\mathbf{G}_3(t))\mathbf{G}_3(t) - (\mathfrak{u} + \varpi)\mathbf{G}_1(t)\Big)\mathrm{d}t + \mathrm{d}\mathbf{S}_1(t), \\ \mathrm{d}\mathbf{G}_2(t) = \Big(\varpi\mathbf{G}_1(t) - \beta_2\mathcal{H}_2(\mathbf{G}_2(t),\mathbf{G}_3(t))\mathbf{G}_3(t) - (\mathfrak{u} + \varsigma)\mathbf{G}_2(t)\Big)\mathrm{d}t + \mathrm{d}\mathbf{S}_2(t), \\ \mathrm{d}\mathbf{G}_3(t) = \Big(\beta_1\mathcal{H}_1(\mathbf{G}_1(t),\mathbf{G}_3(t))\mathbf{G}_3(t) + \beta_2\mathcal{H}_2(\mathbf{G}_2(t),\mathbf{G}_3(t))\mathbf{G}_3(t) - (\mathfrak{u} + \mathfrak{a} + \mathfrak{c})\mathbf{G}_3(t)\Big)\mathrm{d}t + \mathrm{d}\mathbf{S}_3(t). \end{cases} \tag{6}$$

In this case, we set

$$\mathbb{R}_{+}^{3,\star} = \{(z_1, z_2, z_3) : \ z_1 > 0, z_2 > 0, z_3 > 0\},$$

and we simply survey the long-run conduct of the first three groups.

Theorem 1. *Assume that $\mathfrak{R}_0^{\star} > 0$ holds. Then, system (6) admits a single ergodic steady distribution $\pi^{\star}(\cdot)$.*

Biological interpretation 1. The ergodicity reveals that the perturbed model (2) has a limiting stable distribution that prophesies the continuation of the infection. This means that the infected group will tend to stay for a long time.

Proof. See Appendix B. □

Remark 4. *From Lemma 2 and Theorem 1, we can establish more indications on the insistence of the stochastic processes $\mathbf{G}_1$, $\mathbf{G}_2$, $\mathbf{G}_4$ and $\mathbf{G}_4$. Specifically, we obtain*

$$\lim_{t\to\infty} t^{-1} \int_0^t \mathbf{G}_1(\tau)\mathrm{d}\tau = \int_{\mathbb{R}_{+}^{4,\star}} c_1 \pi^{\star}(\mathrm{d}c_1, \mathrm{d}c_2, \mathrm{d}c_3, \mathrm{d}c_4) < \infty,$$
$$\lim_{t\to\infty} t^{-1} \int_0^t \mathbf{G}_2(\tau)\mathrm{d}\tau = \int_{\mathbb{R}_{+}^{4,\star}} c_2 \pi^{\star}(\mathrm{d}c_1, \mathrm{d}c_2, \mathrm{d}c_3, \mathrm{d}c_4) < \infty,$$
$$\lim_{t\to\infty} t^{-1} \int_0^t \mathbf{G}_3(\tau)\mathrm{d}\tau = \int_{\mathbb{R}_{+}^{4,\star}} c_3 \pi^{\star}(\mathrm{d}c_1, \mathrm{d}c_2, \mathrm{d}c_3, \mathrm{d}c_4) < \infty,$$
$$\lim_{t\to\infty} t^{-1} \int_0^t \mathbf{G}_4(\tau)\mathrm{d}\tau = \int_{\mathbb{R}_{+}^{4,\star}} c_4 \pi^{\star}(\mathrm{d}c_1, \mathrm{d}c_2, \mathrm{d}c_3, \mathrm{d}c_4) < \infty.$$

By way of explanation, this shows the continuation of all groups of the population.

3.2. The Disappearance Case

Theorem 2. *If $\mathfrak{R}_0^{\star} < 0$, then $\mathbf{G}_3$ verifies that*

$$\limsup_{t\to\infty} t^{-1} \ \ln \mathbf{G}_3(t) \leq \mathfrak{R}_0^{\star} < 0 \quad \text{(almost surely)},$$

which implies that the group $\mathbf{G}_3(t)$ will disappear with full probability. Furthermore, the distributions of $\mathbf{G}_1(t)$ and $\mathbf{G}_2(t)$ converge (weakly) to the invariant measures $\pi^{\mathbf{S}_1}$ and $\pi^{\mathbf{S}_2}$, respectively.

Biological interpretation 2. The quantity $\mathfrak{R}_0^{\star}$ contains linear random intensities, which are related to the infected class $\mathbf{G}_3$. This designates that if $\mathfrak{R}_0^{\star}$ is strictly less than zero, the stochastic fluctuations help to the inhibition of the illness.

Proof. See Appendix B. □

4. Numerical Verification

This part of the manuscript is devoted to the verification of Theorems 1 and 2 through numerical examples. Through computer simulations, we generated plots for trajectories and histograms, from which the complex dynamical behaviours of the perturbed system (2) can be easily interpreted. Moreover, we chose some reasonable parameter values to verify our hypothetical framework. According to the work presented in [48], we use the following compensated tempered Poisson process:

$$^{i}\mathbb{Y}(t) = \int_0^t \int_{\chi} u \, \widetilde{\mathcal{C}}_i^{\alpha}(\mathrm{d}s, \mathrm{d}u), \quad i = 1, 2, 3, 4, \tag{7}$$

with the associated Lévy measure (4). To numerically apply the method proposed in [29], we define the following setup inputs tuning:

- $(a_j)_{j\geq 1}$ is an i.i.d. Bernoulli random sequence with the associated distribution $\big(\varsigma_{\star,-}/(\varsigma_{\star,-}+\varsigma_{\star,+}), \varsigma_{\star,+}/(\varsigma_{\star,-}+\varsigma_{\star,+})\big)$.
- $(b_j)_{j\geq 1}$ and $(b_j^{'})_{j\geq 1}$ are i.i.d. exponential random variables with the parameter 1, where $B_j = b_1^{'} + \cdots + b_j^{'}$.
- $(c_j)_{j\geq 1}$ are i.i.d. uniform random variables.
- $(d_j)_{j\geq 1}$ is an i.i.d. uniform $U(0,1)$ random sequence.

According to Theorem 5.3 in [29], all of the above sequences are supposed to be mutually independent. Furthermore, the process ${}^{i}\mathbb{Y}$ with (4) can be presented as follows:

- When $0<\alpha<1$, then ${}^{i}\mathbb{Y}(t) = \sum_{j=1}^{\infty} \mathbb{1}_{(0,t]}(c_j)\frac{a_j}{|a_j|}\tilde{S}_1$, for all $0\leq t\leq T$, where $\tilde{S}_1 = \min\left\{ \left(\frac{(\varsigma_{\star,-}+\varsigma_{\star,+})T}{\alpha B_j}\right)^{\frac{1}{\alpha}}, \frac{b_j}{|a_j|}d_j^{\frac{1}{\alpha}} \right\}$.
- When $1\leq\alpha<2$, then ${}^{i}\mathbb{Y}(t) = \sum_{j=1}^{\infty}\left(\mathbb{1}_{(0,t]}(c_j)\frac{a_j}{|a_j|}\tilde{S}_2 - z_0\frac{t}{T}\left(\frac{\varsigma_{\star,-}+\varsigma_{\star,+}}{\alpha j/T}\right)^{\frac{1}{\alpha}}\right) + t\Phi_T$, for all $0\leq t\leq T$ where $\tilde{S}_2 = \min\left\{\left(\frac{\varsigma_{\star,-}+\varsigma_{\star,+}}{\alpha B_j/T}\right)^{\frac{1}{\alpha}}, \frac{b_j}{|a_j|}d_j^{\frac{1}{\alpha}}\right\}$, $z_0 = (\varsigma_{\star,-}-\varsigma_{\star,+})/(\varsigma_{\star,-}+\varsigma_{\star,+})$, $z_1 = \varsigma_{\star,+}\kappa_{\star,+}^{-1-\alpha} - \varsigma_{\star,-}\kappa_{\star,-}^{-1-\alpha}$ and

$$\Phi_T = \begin{cases} \frac{z_0}{T}\zeta_R\left(\frac{1}{\alpha}\right)\left(\frac{T(\varsigma_{\star,-}+\varsigma_{\star,+})}{\alpha}\right)^{\frac{1}{\alpha}} - z_1\Gamma_G(\alpha-1), & 1<\alpha<2, \\ (2\gamma_e + \ln(\varsigma_{\star,-}+\varsigma_{\star,+}))z_1 - \int_{\mathcal{X}} x\ln(|x|)\mathfrak{Z}_\alpha(\mathrm{d}x) & \alpha=1, \end{cases}$$

  where $\zeta_R(\cdot)$ denotes the Riemann zeta function, $\Gamma_G(\cdot)$ is the Gamma function, and γ_e is the Euler constant.

Since the main motive of the tempered α-stable Lévy process is to obtain systems that simulate heavier tails more appropriately compare with the standard Lévy fluctuation, therefore, it is very much important to study the behavior of these tails. First of all, we need to simulate the process ${}^{i}\mathbb{Y}(t)\equiv\mathbb{Y}(t)$ and then we will illustrate the effect of parameter α on the shape of its fluctuations and discontinuities. In Figure 2, we considered four cases for α for understanding the behavior of tails. It was concluded that by choosing a smaller value of α, the jumps become more radical and brutal, while by increasing the value, the trajectories behave like Brownian motion with jumps. In a large time scale, the most recent behavior is clearly visible. Now, we choose $\theta_{iL}(u) = e_{iL}u$ and $\theta_{kQ}(u) = e_{kL}u$, where $e_{iL},\ e_{kQ}>0$, $(i,k=1,2,3,4)$; then, we consider the stochastic system (2) with Beddington-DeAngelis functions as follows:

$$\begin{cases} \mathrm{d}\mathbf{G}_1(t) = \left\{\mathfrak{r}\mathbf{G}_1(t)\left(1-\frac{\mathbf{G}_1(t)}{\mathcal{K}}\right) - \frac{\beta_1\mathbf{G}_1\mathbf{G}_3(t)}{1+\mathfrak{q}_1\mathbf{G}_1+\mathfrak{q}_2\mathbf{G}_3} - (\mathfrak{u}+\varpi)\mathbf{G}_1(t)\right\}\mathrm{d}t + \mathrm{d}\mathbf{S}_1(t), \\ \mathrm{d}\mathbf{G}_2(t) = \left\{\varpi\mathbf{G}_1(t) - \frac{\beta_2\mathbf{G}_2\mathbf{G}_3(t)}{1+\mathfrak{q}_1^\star\mathbf{G}_2+\mathfrak{q}_2^\star\mathbf{G}_3} - (\mathfrak{u}+\varsigma)\mathbf{G}_2(t)\right\}\mathrm{d}t + \mathrm{d}\mathbf{S}_2(t), \\ \mathrm{d}\mathbf{G}_3(t) = \left\{\frac{\beta_1\mathbf{G}_1\mathbf{G}_3(t)}{1+\mathfrak{q}_1\mathbf{G}_1+\mathfrak{q}_2\mathbf{G}_3} + \frac{\beta_2\mathbf{G}_2\mathbf{G}_3(t)}{1+\mathfrak{q}_1^\star\mathbf{G}_2+\mathfrak{q}_2^\star\mathbf{G}_3} - (\mathfrak{u}+\mathfrak{a}+\mathfrak{c})\mathbf{G}_3(t)\right\}\mathrm{d}t + \mathrm{d}\mathbf{S}_3(t), \\ \mathrm{d}\mathbf{G}_4(t) = \left\{\varsigma\mathbf{G}_2(t) + \mathfrak{c}\mathbf{G}_3(t) - \mathfrak{u}\mathbf{G}_4(t)\right\}\mathrm{d}t + \mathrm{d}\mathbf{S}_4(t), \\ \mathbf{G}_1(0)=0.8,\ \mathbf{G}_2(0)=0.1,\ \mathbf{G}_3(0)=0.1,\ \mathbf{G}_4(0)=0.01, \end{cases} \tag{8}$$

where

$$\begin{cases} \mathrm{d}\mathbf{S}_1(t) &= \Big\{\zeta_{1L}\mathbf{G}_1(t) + \zeta_{1Q}\mathbf{G}_1^2(t)\Big\}\mathrm{d}\mathcal{B}_1(t) + \Big\{e_{1L}\mathbf{G}_1(t^-) + e_{1Q}\mathbf{G}_1^2(t^-)\Big\}\mathrm{d}^1\mathbb{Y}(t), \\ \mathrm{d}\mathbf{S}_2(t) &= \Big\{\zeta_{2L}\mathbf{G}_2(t) + \zeta_{2Q}\mathbf{G}_2^2(t)\Big\}\mathrm{d}\mathcal{B}_2(t) + \Big\{e_{2L}\mathbf{G}_2(t^-) + e_{2Q}\mathbf{G}_2^2(t^-)\Big\}\mathrm{d}^2\mathbb{Y}(t), \\ \mathrm{d}\mathbf{S}_3(t) &= \Big\{\zeta_{3L}\mathbf{G}_3(t) + \zeta_{3Q}\mathbf{G}_3^2(t)\Big\}\mathrm{d}\mathcal{B}_3(t) + \Big\{e_{3L}\mathbf{G}_3(t^-) + e_{3Q}\mathbf{G}_3^2(t^-)\Big\}\mathrm{d}^3\mathbb{Y}(t), \\ \mathrm{d}\mathbf{S}_4(t) &= \Big\{\zeta_{4L}\mathbf{G}_4(t) + \zeta_{4Q}\mathbf{G}_4^2(t)\Big\}\mathrm{d}\mathcal{B}_4(t) + \Big\{e_{4L}\mathbf{G}_4(t^-) + e_{4Q}\mathbf{G}_4^2(t^-)\Big\}\mathrm{d}^4\mathbb{Y}(t). \end{cases}$$

For simplicity, we will present advanced simulation results for system (8) in the case of the single-sided tempered stable processes ${}^i\mathbb{Y}(t)$ with $\varsigma_{\star,-} = 0$. The deterministic parameters of (8) are as follows: $\mathfrak{r} = 0.04$, $\mathcal{K} = 1$, $\beta_1 = 0.1$, $\mathfrak{q}_1 = 0.15$, $\mathfrak{q}_2 = 0.12$, $\mathfrak{u} = 0.01$, $\varpi = 0.01$, $\beta_2 = 0.00045$, $\mathfrak{q}_1^\star = 0.17$, $\mathfrak{q}_2^\star = 0.11$, $\mathfrak{a} = 0.02$, $\mathfrak{c} = 0.0001$, $\varsigma = 0.004$. To study the influence of jumps noises on the dynamics of system (8), we fix the values of the deterministic parameters and will vary the stochastic intensities.

4.1. First Case: $\alpha = 0.7$

4.1.1. Scenario 1: Stationarity and Permanence

Since the proposed algorithm is very sensitive to its inputs, thus we select the intensities of noises from Table 4.

Table 4. Selected values of the noise intensities in system (8) (stationarity case).

Stochastic Parameters	Values
$(\zeta_{1L}, \zeta_{1L}, \zeta_{2L}, \zeta_{3L}, \zeta_{4L})$	(0.051, 0.042, 0.07, 0.0315)
$(\zeta_{1Q}, \zeta_{1Q}, \zeta_{2Q}, \zeta_{3Q}, \zeta_{4Q})$	(0.001, 0.002, 0.004, 0.001)
$(e_{1L}, e_{1L}, e_{2L}, e_{3L}, e_{4L})$	(0.01, 0.011, 0.0101, 0.01025)
$(e_{1Q}, e_{1Q}, e_{2Q}, e_{3Q}, e_{4Q})$	(0.0014, 0.0012, 0.0071, 0.0011)

By choosing a sufficiently large number $T > 0$, the threshold $\mathfrak{R}_0^\star$ is calculated as follows:

$$\begin{aligned} \mathfrak{R}_0^\star = &\int_0^\infty \frac{\beta_1 x}{1+\mathfrak{q}_1 x}\pi^{\mathbf{S}_1}(\mathrm{d}x) + \int_0^\infty \frac{\beta_2 x}{1+\mathfrak{q}_1^\star x}\pi^{\mathbf{S}_2}(\mathrm{d}x) - (\mathfrak{u}+\mathfrak{a}+\mathfrak{c}) \\ &- 0.5\zeta_{3L}^2 - \int_\chi \Big(e_{3L}u - \ln\big(1+e_{3L}u\big)\Big)\mathfrak{Z}_3^{0.7}(\mathrm{d}u). \end{aligned}$$

The probability density functions $\pi^{\mathbf{S}_1}$ and $\pi^{\mathbf{S}_2}$ obey a Fokker–Planck equation, which can be easily approximated through Monte Carlo simulations. Via ergodic property (Lemma 3), we can also estimate these quantities:

$$\lim_{T\to\infty} T^{-1}\int_0^T \frac{\beta_1\mathbf{S}_1(s)}{1+\mathfrak{q}_1\mathbf{S}_1(s)}\mathrm{d}s, \qquad \lim_{T\to\infty} T^{-1}\int_0^T \frac{\beta_2\mathbf{S}_2(s)}{1+\mathfrak{q}_1^\star\mathbf{S}_2(s)}\mathrm{d}s,$$

for a large time T. This last technique is the one we used in our simulations. Since the equations for $\mathbf{S}_1$ and $\mathbf{S}_2$ are disturbed by quadratic α-stable fluctuations, therefore, the said limit will be modified according to the magnitude of the intensities. Consequently, the threshold will also be changed. In this regard, our threshold can expressed as follows:

$$\begin{aligned} \mathfrak{R}_0^\star = &\lim_{T\to\infty}\frac{1}{T}\int_0^T \frac{\beta_1\mathbf{S}_1(s)}{1+\mathfrak{q}_1\mathbf{S}_1(s)}\mathrm{d}s + \lim_{T\to\infty}\frac{1}{T}\int_0^T \frac{\beta_2\mathbf{S}_2(s)}{1+\mathfrak{q}_1^\star\mathbf{S}_2(s)}\mathrm{d}s - (\mathfrak{u}+\mathfrak{a}+\mathfrak{c}) \\ &- 0.5\zeta_{3L}^2 - \int_\chi \Big(e_{3L}u - \ln\big(1+e_{3L}u\big)\Big))\mathfrak{Z}_3^{0.7}(\mathrm{d}u) \\ = &\ 0.0012 > 0. \end{aligned}$$

From Theorem 1, we infer that there is a single steady distribution to system (8). To numerically illustrate this statistical property, we need to present Figure 3, the associated joint two-dimensional densities for all groups. For a good visibility, we offer the upper view of the said joint densities in Figure 4. From numerical approximation and Remark 4, we obtain

$$\begin{aligned}
\lim_{t\to\infty} t^{-1}\int_0^t \mathbf{G}_1(\tau)\mathrm{d}\tau &= \int_{\mathbb{R}_+^{4,\star}} c_1\pi^\star(\mathrm{d}c_1,\mathrm{d}c_2,\mathrm{d}c_3,\mathrm{d}c_4) = 0.3001 > 0,\\
\lim_{t\to\infty} t^{-1}\int_0^t \mathbf{G}_2(\tau)\mathrm{d}\tau &= \int_{\mathbb{R}_+^{4,\star}} c_2\pi^\star(\mathrm{d}c_1,\mathrm{d}c_2,\mathrm{d}c_3,\mathrm{d}c_4) = 0.2060 > 0,\\
\lim_{t\to\infty} t^{-1}\int_0^t \mathbf{G}_3(\tau)\mathrm{d}\tau &= \int_{\mathbb{R}_+^{4,\star}} c_3\pi^\star(\mathrm{d}c_1,\mathrm{d}c_2,\mathrm{d}c_3,\mathrm{d}c_4) = 0.0673 > 0,\\
\lim_{t\to\infty} t^{-1}\int_0^t \mathbf{G}_4(\tau)\mathrm{d}\tau &= \int_{\mathbb{R}_+^{4,\star}} c_4\pi^\star(\mathrm{d}c_1,\mathrm{d}c_2,\mathrm{d}c_3,\mathrm{d}c_4) = 0.0030 > 0.
\end{aligned}$$

This indicates that the infection is still present in the population over time. We talk here about persistence in the mean of the epidemic. In Figure 5, we illustrate the continuation of all groups of the studied population. One can notice that the stochastic trajectories fluctuate around the deterministic solution with reasonable distances according to magnitude of the noises.

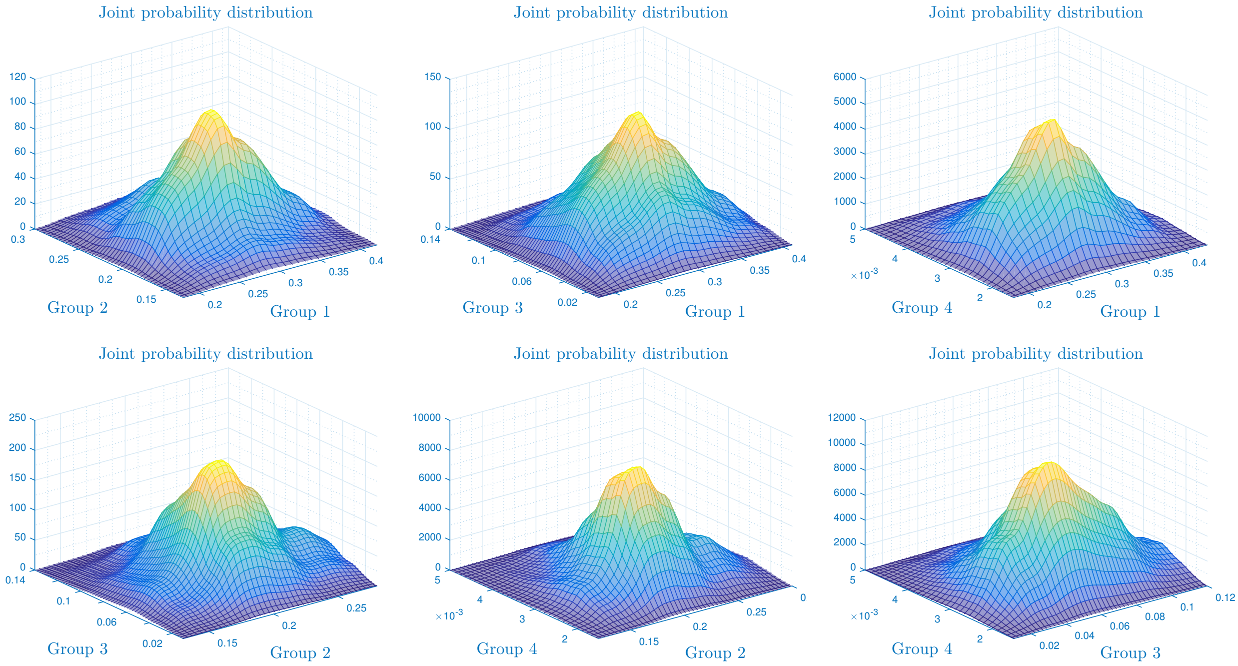

Figure 3. The 3D representation of the joint densities at time $t = 5000$ of system (8) with stochastic parameters appearing in Scenario 1, different colored stages indicate various sizes of the density.

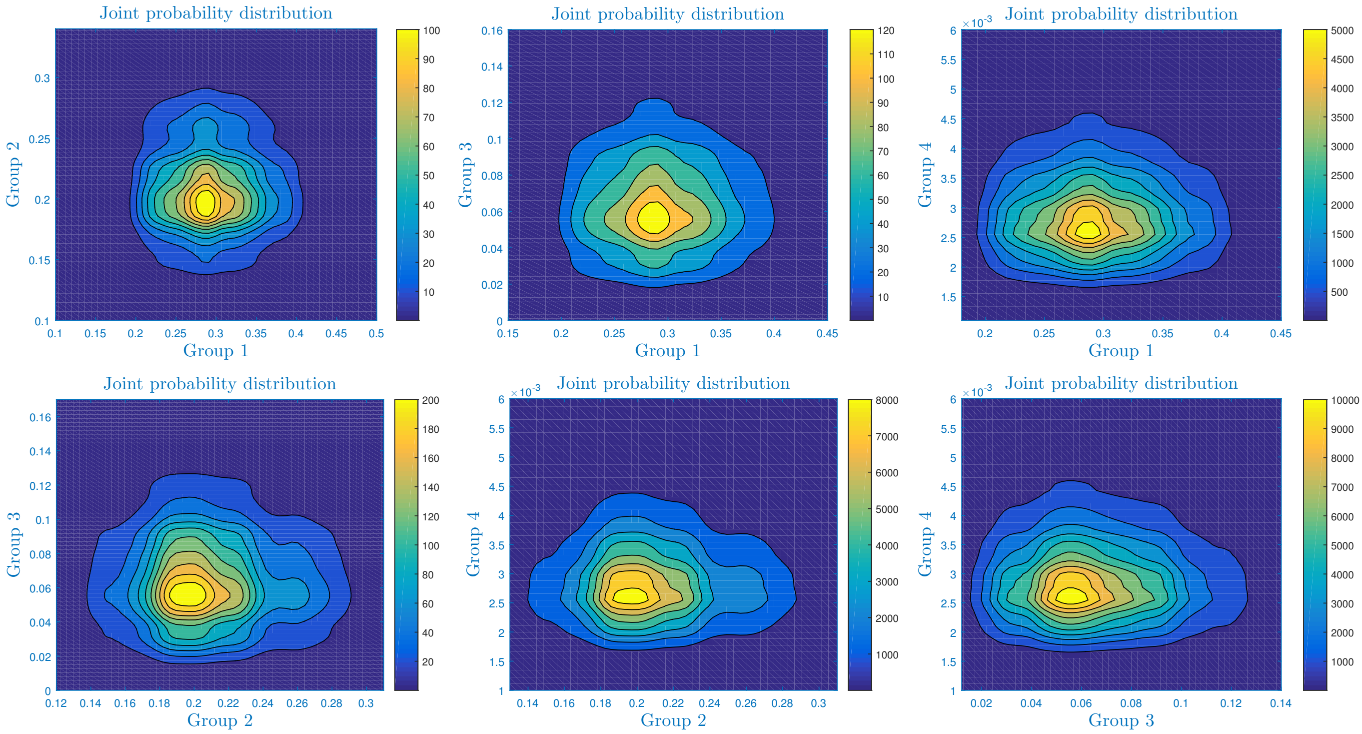

Figure 4. The 2D upper view of the joint densities at time $t = 5000$ of the classes $\mathbf{G}_1$, $\mathbf{G}_2$, $\mathbf{G}_3$ and $\mathbf{G}_4$.

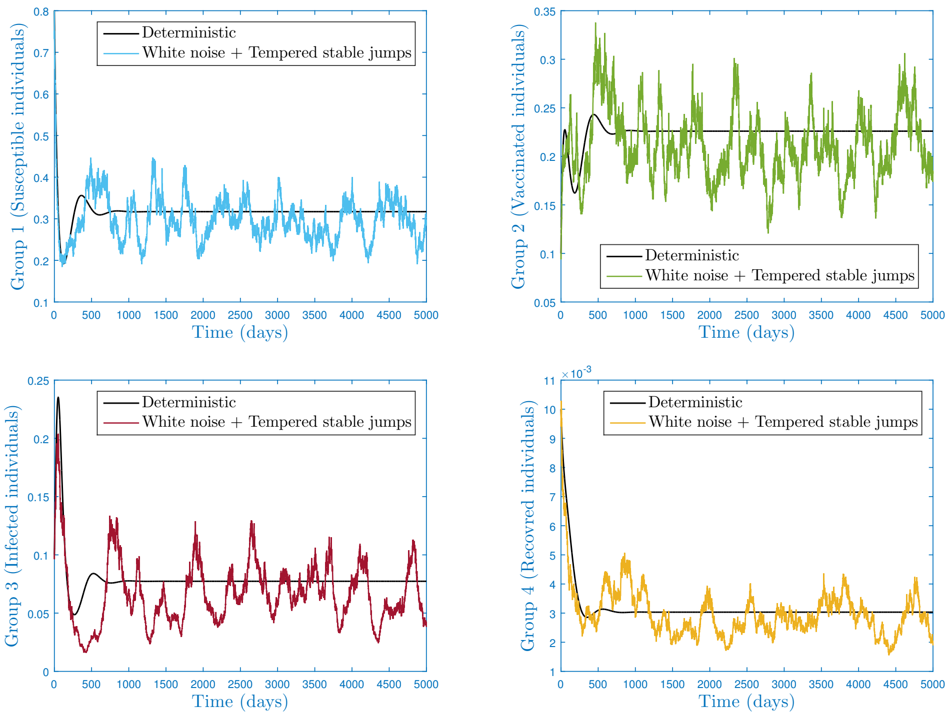

Figure 5. Computer simulations based on the probabilistic model (8) with tempered α-stable jumps. The deterministic parameters are selected as follows: $\mathfrak{r} = 0.04$, $\mathcal{K} = 1$, $\beta_1 = 0.1$, $\mathfrak{q}_1 = 0.15$, $\mathfrak{q}_2 = 0.12$, $\mathfrak{u} = 0.01$, $\varpi = 0.01$, $\beta_2 = 0.00045$, $\mathfrak{q}_1^\star = 0.17$, $\mathfrak{q}_2^\star = 0.11$, $\mathfrak{a} = 0.02$, $\mathfrak{c} = 0.0001$, $\varsigma = 0.004$. The deterministic parameters are chosen from Table 4.

4.1.2. Scenario 2: Extinction

Now, we seek to verify that the long-term dynamics of the model can change its behavior at certain noise intensities. To this end, we increase the amplitude of the noises as stated in Table 5.

Table 5. Selected values of the noise intensities in system (8) (extinction case).

Stochastic Parameters	*Values*
$(\zeta_{1L}, \zeta_{1L}, \zeta_{2L}, \zeta_{3L}, \zeta_{4L})$	(0.11, 0.104, 0.12, 0.08)
$(\zeta_{1Q}, \zeta_{1Q}, \zeta_{2Q}, \zeta_{3Q}, \zeta_{4Q})$	(0.01, 0.01, 0.01, 0.01)
$(e_{1L}, e_{1L}, e_{2L}, e_{3L}, e_{4L})$	(0.1, 0.1, 0.201, 0.125)
$(e_{1Q}, e_{1Q}, e_{2Q}, e_{3Q}, e_{4Q})$	(0.01, 0.01, 0.01, 0.01)

A numerical calculation gives

$$\begin{aligned}\mathfrak{R}_0^\star &= \lim_{T\to\infty}\frac{1}{T}\int_0^T \frac{\beta_1\mathbf{S}_1(s)}{1+\mathfrak{q}_1\mathbf{S}_1(s)}\mathrm{d}s + \lim_{T\to\infty}\frac{1}{T}\int_0^T \frac{\beta_2\mathbf{S}_2(s)}{1+\mathfrak{q}_1^\star\mathbf{S}_2(s)}\mathrm{d}s - (\mathfrak{u}+\mathfrak{a}+\mathfrak{c}) \\ &\quad - 0.5\zeta_{3L}^2 - \int_\chi \Big(e_{3L}u - \ln\big(1+e_{3L}u\big)\Big))\mathfrak{z}_3^{0.7}(\mathrm{d}u) \\ &= -0.0047 < 0.\end{aligned}$$

In accordancewith Theorem 2, the sign of the threshold indicates that we have passed from the case of permanence to the phenomenon of extinction. From Figure 6, we notice that the stochastic trajectory of group 3 is extinguished after a given time while the deterministic solution still continues. It's so logical because we didn't change the deterministic parameters and we just made some modifications on the intensity of the noises. Therefore, we deduce that stochastic fluctuations have a passive influence on the long-term behavior of the infection and can modify the bifurcation of the proposed system.

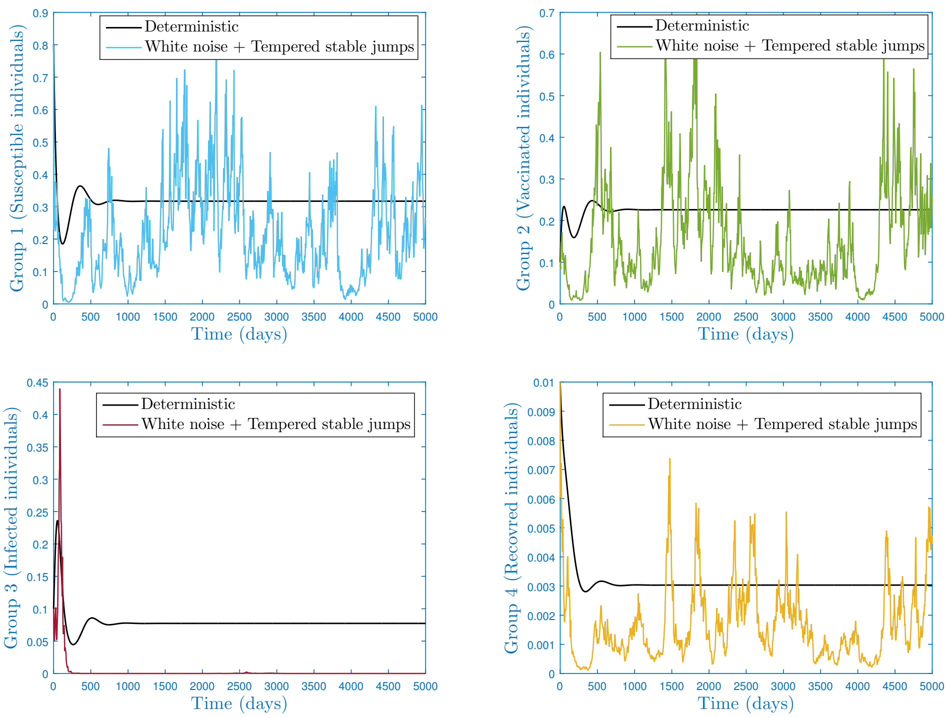

Figure 6. Computer simulations based on the probabilistic model (8) with tempered α-stable jumps. The deterministic parameters are selected as follows: $\mathfrak{r} = 0.04$, $\mathcal{K} = 1$, $\beta_1 = 0.1$, $\mathfrak{q}_1 = 0.15$, $\mathfrak{q}_2 = 0.12$, $\mathfrak{u} = 0.01$, $\varpi = 0.01$, $\beta_2 = 0.00045$, $\mathfrak{q}_1^\star = 0.17$, $\mathfrak{q}_2^\star = 0.11$, $\mathfrak{a} = 0.02$, $\mathfrak{c} = 0.0001$, $\varsigma = 0.004$. The fixed deterministic coefficients are chosen from Table 5.

4.2. Second Case: $\alpha = 1.7$

4.2.1. Scenario 1: Stationarity and Permanence

To exhibit this behavior of the model, we leave the deterministic parameters unchanged and will choose the stochastic parameters from Table 4. The main purpose is to ensure that

Theorem 1 is valid in the case of $\alpha \in [1,2)$ and also to investigate the impact of a high value of α on the shape of fluctuations and tails. From Figure 7, we show that unlike the case of $\alpha \in (0,1)$, the stochastic trajectories do not fluctuate around a deterministic solution. In fact, they move away from the steady state with long tails, which indicates that the increase in the value of α leads to the worsening of the endemic situation. For clarity of visualization, we present Figures 8 and 9 having various plots of joint density functions associated with all groups. Therefore, we numerically verified the continuation of infection in the population. Regarding the effect of the parameter α on the mean averages of the processes $\mathbf{G}_i$ $(i = 1,2,3,4)$, we have

$$\begin{aligned}
\lim_{t\to\infty} t^{-1}\int_0^t \mathbf{G}_1(\tau)\mathrm{d}\tau &= \int_{\mathbb{R}_+^{4,\star}} c_1\pi^\star(\mathrm{d}c_1,\mathrm{d}c_2,\mathrm{d}c_3,\mathrm{d}c_4) = 0.5236\uparrow,\\
\lim_{t\to\infty} t^{-1}\int_0^t \mathbf{G}_2(\tau)\mathrm{d}\tau &= \int_{\mathbb{R}_+^{4,\star}} c_2\pi^\star(\mathrm{d}c_1,\mathrm{d}c_2,\mathrm{d}c_3,\mathrm{d}c_4) = 0.3879\uparrow,\\
\lim_{t\to\infty} t^{-1}\int_0^t \mathbf{G}_3(\tau)\mathrm{d}\tau &= \int_{\mathbb{R}_+^{4,\star}} c_3\pi^\star(\mathrm{d}c_1,\mathrm{d}c_2,\mathrm{d}c_3,\mathrm{d}c_4) = 0.1145\uparrow,\\
\lim_{t\to\infty} t^{-1}\int_0^t \mathbf{G}_4(\tau)\mathrm{d}\tau &= \int_{\mathbb{R}_+^{4,\star}} c_4\pi^\star(\mathrm{d}c_1,\mathrm{d}c_2,\mathrm{d}c_3,\mathrm{d}c_4) = 0.0048\uparrow.
\end{aligned}$$

This shows that by increasing the value of α implies the rise in the average value of all groups.

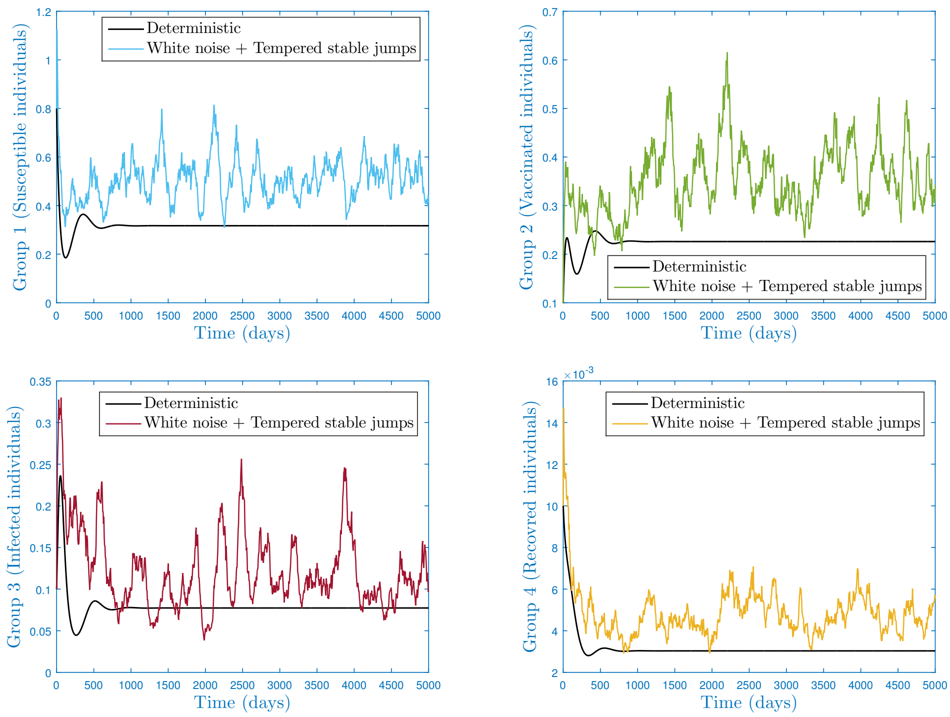

Figure 7. Computer simulations obtained by simulating the probabilistic model (8) with tempered α-stable jumps. The deterministic parameters are selected as follows: $\mathfrak{r} = 0.04$, $\mathcal{K} = 1$, $\beta_1 = 0.1$, $\mathfrak{q}_1 = 0.15$, $\mathfrak{q}_2 = 0.12$, $\mathfrak{u} = 0.01$, $\varpi = 0.01$, $\beta_2 = 0.00045$, $\mathfrak{q}_1^\star = 0.17$, $\mathfrak{q}_2^\star = 0.11$, $\mathfrak{a} = 0.02$, $\mathfrak{c} = 0.0001$, $\varsigma = 0.004$. The fixed deterministic coefficients are chosen from Table 4.

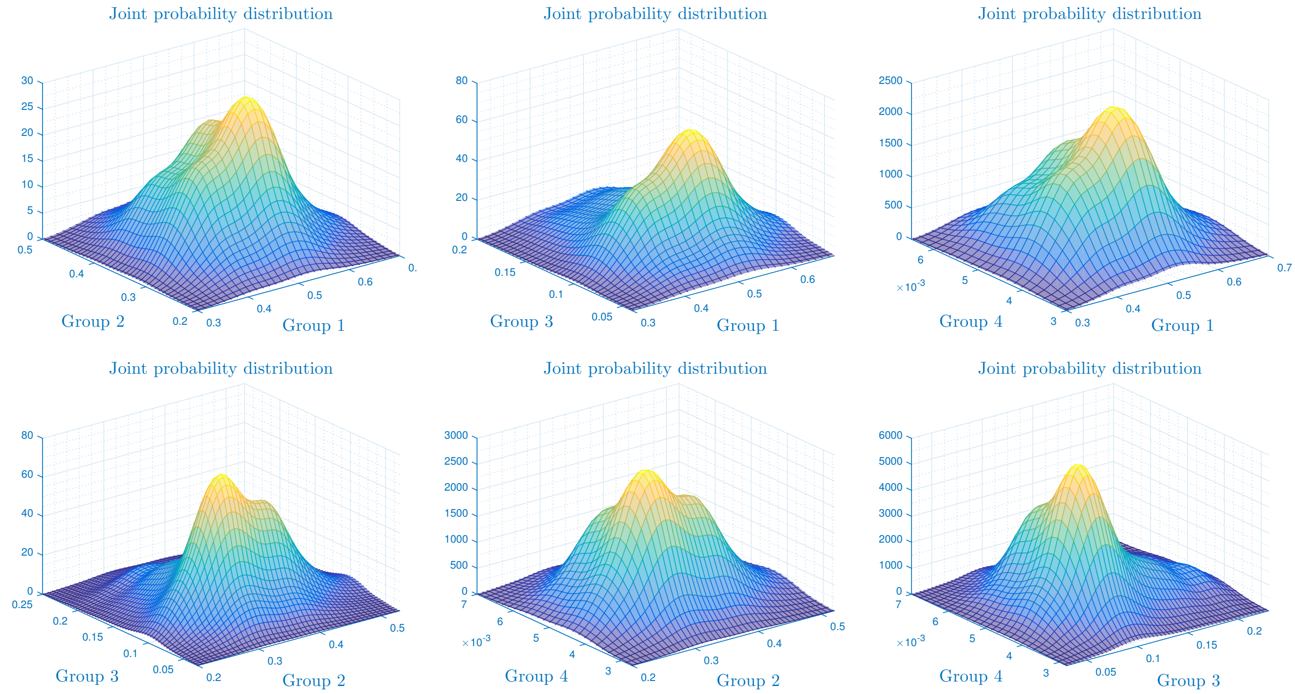

Figure 8. The 3D representation of the joint densities at time $t = 5000$ of system (8) with stochastic parameters appearing in Scenario 1, different colors indicates various sizes of the density.

4.2.2. Scenario 2: Extinction

Again, we keep the deterministic parameters as that was in previous cases and we choose the stochastic parameters from Table 5. Here, the main goal is to validate the conclusion of Theorem 2 in the case of $\alpha \in [1, 2)$. Figure 10 illustrates the case of high values of α and noises. One can notice that the jumps are long and the stochastic trajectories of group 1, 2, 4 fluctuate outside the deterministic solution, while the trajectory of group 3 disappears.

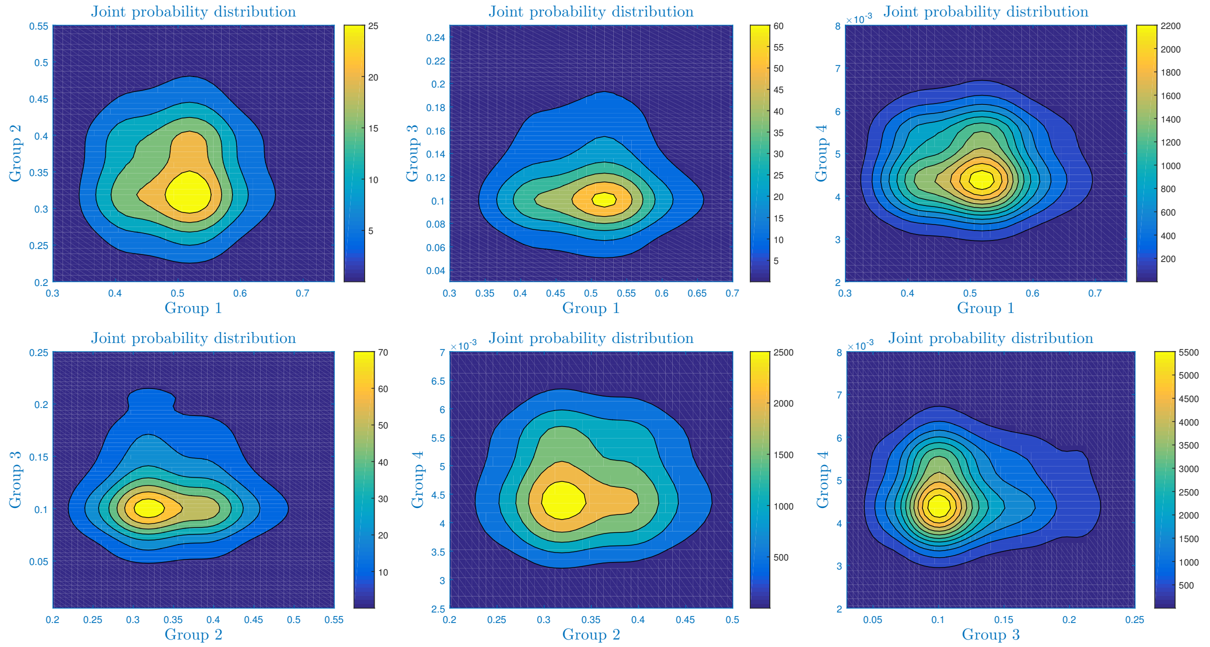

Figure 9. Numerical illustration of the 2D upper view of the joint densities at time $t = 5000$ of the groups $\mathbf{G}_1$, $\mathbf{G}_2$, $\mathbf{G}_3$ and $\mathbf{G}_4$. We remark that the stationary processes follow the footsteps of limit distributions, and the ergodic property is satisfied.

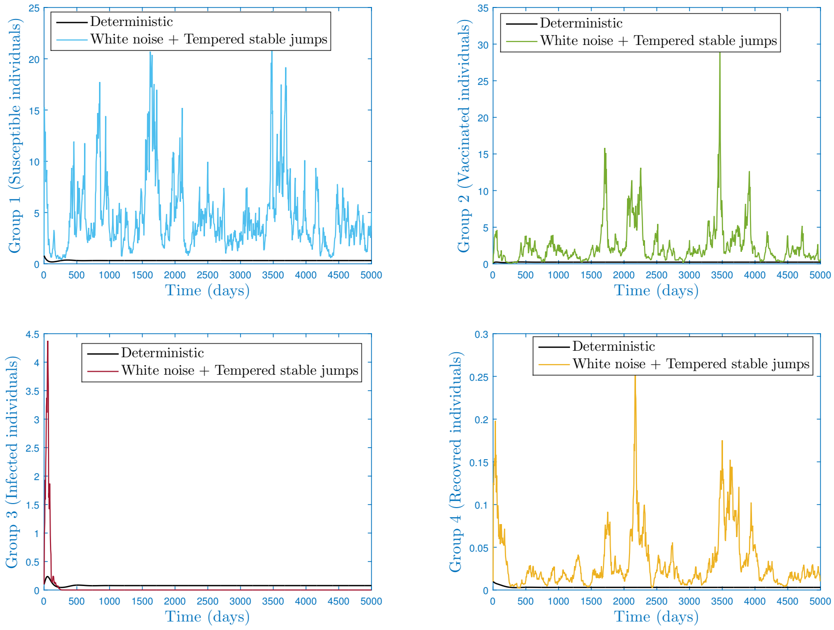

Figure 10. Computer simulation based on the probabilistic model (8) with tempered α-stable jumps. The deterministic parameters are selected as follows: $\mathfrak{r} = 0.04$, $\mathcal{K} = 1$, $\beta_1 = 0.1$, $\mathfrak{q}_1 = 0.15$, $\mathfrak{q}_2 = 0.12$, $\mathfrak{u} = 0.01$, $\varpi = 0.01$, $\beta_2 = 0.00045$, $\mathfrak{q}_1^\star = 0.17$, $\mathfrak{q}_2^\star = 0.11$, $\mathfrak{a} = 0.02$, $\mathfrak{c} = 0.0001$, $\varsigma = 0.004$. The deterministic parameters are chosen from Table 5.

4.3. The Influence of Parameter α on the Form of the Probability Density Function

In the previous two parts of this section, we numerically investigated the long-run bifurcation (LR-bifurcation). In this part, we show the long-rung modal bifurcation (LRM-bifurcation), which mainly depicts the geometric variations in the form of the steady probability density function associated with the dynamical system. Specifically, we numerically analyze the influence of parameter α on the form of the probability density function. Figure 11 suggest that the parameter α have a significant role in changing the shape of the stationary distribution associated with model (8). For example, in the case of $\mathbf{G}_1$, we show that the density function changes its support from $\alpha = 1.98$ to $\alpha = 0.25$. We can justify that when α takes a high value, the stochastic trajectories characterizes by the huge fluctuations and jumps. However, if α is small, the stochastic trajectories concentrate around the endemic equilibrium.

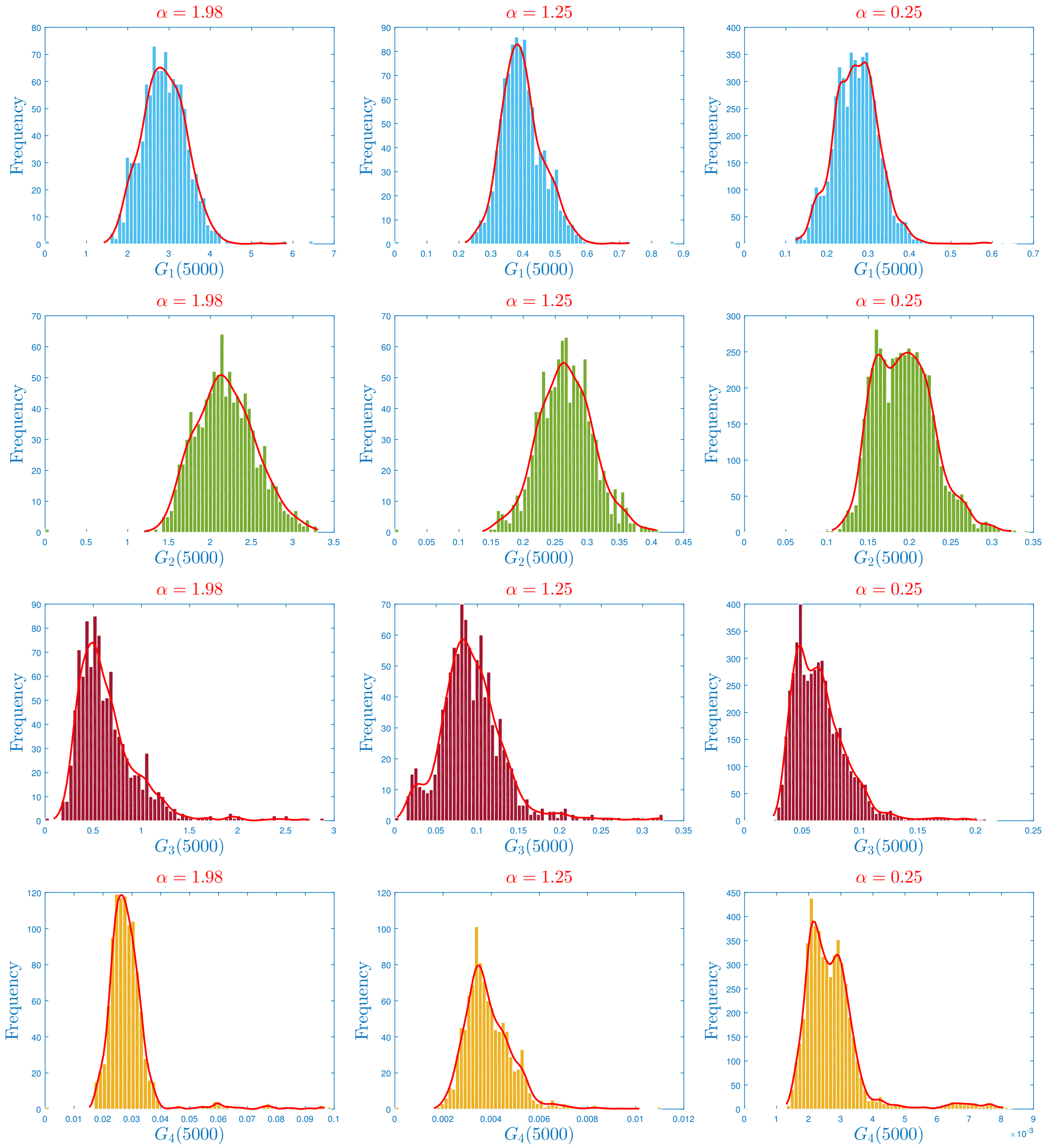

Figure 11. The associated frequency histograms at time $t = 5000$ and the approximated density functions of groups $\mathbf{G}_1$, $\mathbf{G}_2$, $\mathbf{G}_3$, $\mathbf{G}_4$. The fixed deterministic coefficients are selected as follows: $\mathfrak{r} = 0.04$, $\mathcal{K} = 1$, $\beta_1 = 0.1$, $\mathfrak{q}_1 = 0.15$, $\mathfrak{q}_2 = 0.12$, $\mathfrak{u} = 0.01$, $\varpi = 0.01$, $\beta_2 = 0.00045$, $\mathfrak{q}_1^{\star} = 0.17$, $\mathfrak{q}_2^{\star} = 0.11$, $\mathfrak{a} = 0.02$, $\mathfrak{c} = c = 0.0001$, $\varsigma = 0.004$. The fixed deterministic coefficients are selected from Table 4.

5. Conclusions

This research proposed a new approach to dealing with an epidemic model under real and interesting hypotheses. We have proposed and investigated a new form of the SVIR system that accounts for two major improvements: the general response functions and the independent quadratic tempered α-stable Lévy noises. This integration gives a global perspective of the interaction between various parts of the population in a highly disrupted environment. The findings of this paper can be summarized as follows:

- We determined the novel model's global threshold using some dynamical properties of a two-block boundary system (5) perturbed by quadratic tempered α-stable Lévy noises.

- In Theorem 1, we proved a few results related to the stationarity and ergodicity of the system. It is worthy to mention that the analysis of these long-term properties is very significant for the underlying perturbed systems, especially in case of epidemiological models where the ergodicity offers a general idea of the infection permanence.
- In Theorem 2, we studied the extinction case and the weak convergence of susceptible and vaccinated distributions to that of the two-block boundary system (5).
- In the numerical simulation part, we have ensured the accuracy of our threshold. Further, we explored the impact of noise and α on the infection's dynamics. In particular, we showed that jumps have a negative influence on the long-term behavior of the disease in the sense that they lead to complete extinction. Furthermore, it was discovered that parameter α had a significant impact on the shape of the stationary distribution.

In general, we pointed out that this study generalises many previous works to the case of quadratic Lévy jumps. Furthermore, it offers new insights into understanding disease spread with complex real-world assumptions. In other words, the technique outlined in this article opens up several prospects for further investigation.

Author Contributions: Formal analysis, Y.S. and A.D.; Funding acquisition, A.K.; Investigation, Y.S., A.D. and M.T.; Methodology, Y.S., A.D. and M.T.; Project administration, A.D. and A.K.; Resources, A.K.; Software, A.D. and Y.S.; Writing—original draft, Y.S. and A.D.; Writing—review & editing, A.K. and M.T. All authors have read and agreed to the published version of the manuscript.

Funding: This research was sponsored by the Guangzhou Government Project under Grant No. 62216235, and the National Natural Science Foundation of China (Grant No. 12250410247).

Informed Consent Statement: Not applicable.

Data Availability Statement: The data used to support the findings of this study are already included in the article.

Conflicts of Interest: The authors declare no conflict of interest.

Appendix A. Proof of Lemma 4

By employing Itô's lemma for Itô-Lévy processes [49], we get

$$
\begin{aligned}
\mathrm{d}\ln \mathbf{S}_1(t) = \Bigg\{ \Big(\overbrace{\mathfrak{r} - (\mathfrak{u} + \varpi)}^{=\eta^{\star\star}} \Big) - \frac{\mathfrak{r}\mathbf{S}_1(t)}{\mathcal{K}} - 0.5\big(\zeta_{1L} + \zeta_{1Q}\mathbf{S}_1(t)\big)^2 \\
+ \int_{\chi} \Big(\ln\big(1 + \theta_{1L}(u) + \theta_{1Q}(u)\mathbf{S}_1(t)\big) - \big(\theta_{1L}(u) + \theta_{1Q}(u)\mathbf{S}_1(t)\big) \Big) \mathfrak{Z}_1^{\alpha}(\mathrm{d}u) \Bigg\} \mathrm{d}t \\
+ \big(\zeta_{1L} + \zeta_{1Q}\mathbf{S}_1(t)\big)\mathrm{d}\mathcal{B}_1(t) + \int_{\chi} \ln\big(1 + \theta_{1L}(u) + \theta_{1Q}(u)\mathbf{S}_1(t^-)\big)\widetilde{\mathcal{C}}_1^{\alpha}(\mathrm{d}t, \mathrm{d}u).
\end{aligned}
$$

We integrate the above relation from 0 to t and dividing both sides by t gives

$$
\begin{aligned}
&\frac{\ln \mathbf{S}_1(t) - \ln \mathbf{S}_1(0)}{t} \\
&\leq \eta^{\star\star} - \frac{\mathfrak{r}}{\mathcal{K}} \int_0^t \mathbf{S}_1(s)\mathrm{d}s - 0.5\zeta_{1L}^2 - \int_{\chi} \Big(\theta_{1L}(u) - \ln\big(1 + \theta_{1L}(u)\big) \Big) \mathfrak{Z}_1^{\alpha}(\mathrm{d}u) - \frac{\zeta_{1L}\zeta_{1Q}}{t} \int_0^t \mathbf{S}_1(s)\mathrm{d}s \\
&\quad - \frac{0.5\zeta_{1Q}^2}{t} \int_0^t \mathbf{S}_1^2(s)\mathrm{d}s + \frac{1}{t} \int_0^t \zeta_{1L}\mathrm{d}\mathcal{B}_1(s) \\
&\quad + \frac{1}{t} \int_0^t \int_{\chi} \left[\ln\left(1 + \frac{\theta_{1Q}(u)\mathbf{S}_1(s)}{1 + \theta_{1L}(u)}\right) - \theta_{1Q}(u)\mathbf{S}_1(s) \right] \mathfrak{Z}_1^{\alpha}(\mathrm{d}u)\mathrm{d}s \\
&\quad + \frac{1}{t} \int_0^t \zeta_{1Q}\mathbf{S}_1(s)\mathrm{d}\mathcal{B}_1(s) + \frac{1}{t} \int_0^t \int_{\chi} \ln\big(1 + \theta_{1L}(u)\big)\widetilde{\mathcal{C}}_1^{\alpha}(\mathrm{d}s, \mathrm{d}u) \\
&\quad + \frac{1}{t} \int_0^t \int_{\chi} \ln\left(1 + \frac{\theta_{1Q}(u)\mathbf{S}_1(s^-)}{1 + \theta_{1L}(u)}\right)\widetilde{\mathcal{C}}_1^{\alpha}(\mathrm{d}s, \mathrm{d}u).
\end{aligned}
$$

We let $\mathcal{Q}_1(t) = \int_0^t \zeta_{1L} \mathrm{d}\mathcal{B}_1(s)$ and $\mathcal{Q}_2(t) = \int_0^t \int_\chi \ln\left(1+\theta_{1L}(u)\right)\widetilde{\mathcal{C}}_1^\alpha(\mathrm{d}s, \mathrm{d}u)$. It is easy to show that their quadratic variations are given by

$$\langle \mathcal{Q}_1(t), \mathcal{Q}_1(t)\rangle = \zeta_{1L}^2 t \quad \text{and} \quad \langle \mathcal{Q}_2(t), \mathcal{Q}_2(t)\rangle = t\int_\chi \Big(\ln\left(1+\theta_{1L}(u)\right)\Big)^2 \mathfrak{Z}_1^\alpha(\mathrm{d}u).$$

By employing the theorem of strong large numbers [50], we obtain $t^{-1}\ \mathcal{Q}_1(t)$ and $t^{-1}\ \mathcal{Q}_2(t)$ converge almost surely to zero as t goes to ∞. Now, we apply the exponential inequality introduced in [50], then

$$\begin{aligned}\mathbb{P}_\Omega\Bigg\{ \sup_{0\le t\le \mathfrak{n}} \Bigg[\int_0^t \zeta_{1Q}\mathbf{S}_1(s)\mathrm{d}\mathcal{B}_1(s) - 0.5\int_0^t \zeta_{1Q}^2 \mathbf{S}_1^2(s)\mathrm{d}s \\ - \int_0^t\int_\chi \left(\left(\frac{\theta_{1Q}(u)\mathbf{S}_1(s)}{1+\theta_{1L}(u)}\right) + \ln\left(1+\frac{\theta_{1Q}(u)\mathbf{S}_1(s)}{1+\theta_{1L}(u)}\right)\right)\mathfrak{Z}_1^\alpha(\mathrm{d}u)\mathrm{d}s \\ + \int_0^t\int_\chi \ln\left(1+\frac{\theta_{1Q}(u)\mathbf{S}_1(s^-)}{1+\theta_{1L}(u)}\right)\widetilde{\mathcal{C}}_1^\alpha(\mathrm{d}s,\mathrm{d}u)\Bigg] \ge 2\ln\mathfrak{n}\Bigg\} \le \frac{1}{\mathfrak{n}^2}.\end{aligned}$$

On the other hand, Borel-Cantelli Lemma [50] states that for almost $\omega \in \Omega$, we have the existence of an integer $\mathfrak{n}_\omega > 0$ such that for all $n \ge \mathfrak{n}_\omega$, $t \in [-1+\mathfrak{n}, \mathfrak{n})$ a.s.,

$$\begin{aligned}&2\ln\mathfrak{n} + 0.5\int_0^t \zeta_{1Q}^2\mathbf{S}_1^2(s)\mathrm{d}s + \int_0^t\int_\chi \left(\left(\frac{\theta_{1Q}(u)\mathbf{S}_1(s)}{1+\theta_{1L}(u)}\right) - \ln\left(1+\frac{\theta_{1Q}(u)\mathbf{S}_1(s)}{1+\theta_{1L}(u)}\right)\right)\mathfrak{Z}_1^\alpha(\mathrm{d}u)\mathrm{d}s \\ &\ge \int_0^t \zeta_{1Q}\mathbf{S}_1(s)\mathrm{d}\mathcal{B}_1(s) + \int_0^t\int_\chi \ln\left(1+\frac{\theta_{1Q}(u)\mathbf{S}_1(s^-)}{1+\theta_{1L}(u)}\right)\widetilde{\mathcal{C}}_1^\alpha(\mathrm{d}s,\mathrm{d}u).\end{aligned}$$

Consequently, for all $\mathfrak{n} \ge \mathfrak{n}_\omega$, $t \in [\mathfrak{n}-1, \mathfrak{n}) \subseteq \mathbb{R}_+$ a.s., we established that

$$\begin{aligned}\frac{\ln\mathbf{S}_1(t) - \ln\mathbf{S}_1(0)}{t} \le& \left\{\eta^{\star\star} - \frac{\mathfrak{r}}{\mathcal{K}t}\int_0^t \mathbf{S}_1(s)\mathrm{d}s - \frac{\zeta_{1L}\zeta_{1Q}}{t}\int_0^t \mathbf{S}_1(s)\mathrm{d}s - 0.5\zeta_{1L}^2 - \int_\chi \Big(\theta_{1L}(u) - \ln\left(1+\theta_{1L}(u)\right)\Big)\mathfrak{Z}_1^\alpha(\mathrm{d}u)\right\} \\ &+ \frac{1}{t}\int_0^t\int_\chi \left(\left(\frac{\theta_{1Q}(u)\mathbf{S}_1(s)}{1+\theta_{1L}(u)}\right) - \theta_{1Q}(u)\mathbf{S}_1(s)\right)\mathfrak{Z}_1^\alpha(\mathrm{d}u)\mathrm{d}s + \frac{\mathcal{Q}_1(t)}{t} + \frac{\mathcal{Q}_2(t)}{t} + \frac{2\ln\mathfrak{n}}{\mathfrak{n}-1}.\end{aligned}$$

$$\begin{aligned}\frac{1}{t}\int_0^t \mathbf{S}_1(s)\mathrm{d}s \le& \frac{\mathcal{K}}{(\mathfrak{r}+\mathcal{K}\zeta_{1L}\zeta_{1Q})}\left\{\eta^{\star\star} - 0.5\zeta_{1L}^2 - \int_\chi \Big(\theta_{1L}(u) - \ln\left(1+\theta_{1L}(u)\right)\Big)\mathfrak{Z}_1^\alpha(\mathrm{d}u)\right\} \\ &+ \frac{\mathcal{K}}{(\mathfrak{r}+\mathcal{K}\zeta_{1L}\zeta_{1Q})}\left\{\frac{1}{t}\int_0^t\int_\chi \left(\left(\frac{\theta_{1Q}(u)\mathbf{S}_1(s)}{1+\theta_{1L}(u)}\right) - \theta_{1Q}(u)\mathbf{S}_1(s)\right)\mathfrak{Z}_1^\alpha(\mathrm{d}u)\mathrm{d}s \right. \\ &\left. + \frac{\mathcal{Q}_1(t)}{t} + \frac{\mathcal{Q}_2(t)}{t} + \frac{2\ln\mathfrak{n}}{\mathfrak{n}-1}\right\} \\ &+ \frac{\mathcal{K}}{(\mathfrak{r}+\mathcal{K}\zeta_{1L}\zeta_{1Q})}\left\{\frac{\ln\mathbf{S}_1(t) - \ln\mathbf{S}_1(0)}{t}\right\}.\end{aligned}$$

By taking the limit on both sides of the last result, we have

$$\lim_{t\to\infty}\frac{1}{t}\int_0^t \mathbf{S}_1(s)\mathrm{d}s \le \frac{\mathcal{K}}{(\mathfrak{r}+\mathcal{K}\zeta_{1L}\zeta_{1Q})}\left\{\eta^{\star\star} - 0.5\zeta_{1L}^2 - \int_\chi \Big(\theta_{1L}(u) - \ln\left(1+\theta_{1L}(u)\right)\Big)\mathfrak{Z}_1^\alpha(\mathrm{d}u)\right\} = \varphi_1^{\mathbf{S}} > 0.$$

To establish the second estimation, we simply take the expectation on both sides of the second block of (5), thus we have

$$\begin{aligned} 0 = \lim_{t\to\infty}\frac{\mathbb{E}_{\{\Omega,\mathbb{P}\}}\mathbf{S}_2(t)}{t} &= \varpi\lim_{t\to\infty}\frac{1}{t}\int_0^t \mathbb{E}_{\{\Omega,\mathbb{P}\}}\mathbf{S}_1(s)\mathrm{d}s - (\mathfrak{u}+\varsigma)\lim_{t\to\infty}\frac{1}{t}\int_0^t \mathbb{E}_{\{\Omega,\mathbb{P}\}}\mathbf{S}_2(s)\mathrm{d}s \\ &= \varpi\mathbb{E}_{\{\Omega,\mathbb{P}\}}\lim_{t\to\infty}\frac{1}{t}\int_0^t \mathbf{S}_1(s)\mathrm{d}s - (\mathfrak{u}+\varsigma)\mathbb{E}_{\{\Omega,\mathbb{P}\}}\lim_{t\to\infty}\frac{1}{t}\int_0^t \mathbf{S}_2(s)\mathrm{d}s \\ &\le \varpi\varphi_1^{\mathbf{S}} - (\mathfrak{u}+\varsigma)\mathbb{E}_{\{\Omega,\mathbb{P}\}}\int_{\mathbb{R}_+} x\pi^{\mathbf{S}_2}(\mathrm{d}x) \\ &= \varpi\varphi_1^{\mathbf{S}} - (\mathfrak{u}+\varsigma)\int_{\mathbb{R}_+} x\pi^{\mathbf{S}_2}(\mathrm{d}x). \end{aligned} \tag{A1}$$

Consequently, we get

$$\lim_{t\to\infty}\frac{1}{t}\int_0^t \mathbf{S}_2(s)\mathrm{d}s = \int_{\mathbb{R}_+} x\pi^{\mathbf{S}_2}(\mathrm{d}x) \le \frac{\varpi\varphi_1^{\mathbf{S}}}{(\mathfrak{u}+\varsigma)}.$$

Appendix B. Proof of Theorem 1

From (Lemma 3.2, [51]), we can easily verify that the solution of system (6) has the Feller property. Via employing Itô's formula, we get

$$\begin{aligned} \mathcal{L}\big(-\ln\mathbf{G}_3(t)\big) &= -\beta_1\mathcal{H}_1\big(\mathbf{G}_1(t),\mathbf{G}_3(t)\big) - \beta_2\mathcal{H}_2\big(\mathbf{G}_2(t),\mathbf{G}_3(t)\big) + (\mathfrak{u}+\mathfrak{a}+\mathfrak{c}) + 0.5\big(\zeta_{3L}+\zeta_{3Q}\mathbf{G}_3(t)\big)^2 \\ &\quad - \int_\chi \bigg\{ \ln\Big(1+\theta_{3L}(u)+\theta_{3Q}(u)\mathbf{G}_3(t)\Big) - \Big(\theta_{3L}(u)+\theta_{2Q}(u)\mathbf{G}_3(t)\Big)\bigg\}\mathfrak{Z}_3^\alpha(\mathrm{d}u) \\ &= -\beta_1\mathcal{H}_1\big(\mathbf{S}_1(t),0\big) - \beta_2\mathcal{H}_2\big(\mathbf{S}_2(t),0\big) + (\mathfrak{u}+\mathfrak{a}+\mathfrak{c}) + 0.5\zeta_{3L}^2 \\ &\quad + \int_\chi \Big(\theta_{3L}(u) - \ln\big(1+\theta_{3L}(u)\big)\Big)\mathfrak{Z}_3^\alpha(\mathrm{d}u) \\ &\quad + \beta_1\mathcal{H}_1\big(\mathbf{S}_1(t),0\big) - \beta_1\mathcal{H}_1\big(\mathbf{G}_1(t),\mathbf{G}_3(t)\big) - \beta_1\mathcal{H}_1\big(\mathbf{G}_1(t),0\big) + \beta_1\mathcal{H}_1\big(\mathbf{G}_1(t),0\big) + \beta_2\mathcal{H}_2\big(\mathbf{S}_2(t),0\big) \\ &\quad - \beta_2\mathcal{H}_2\big(\mathbf{G}_2(t),\mathbf{G}_3(t)\big) - \beta_2\mathcal{H}_2\big(\mathbf{G}_2(t),0\big) + \beta_2\mathcal{H}_2\big(\mathbf{G}_2(t),0\big) + \zeta_{3L}\zeta_{3Q}\mathbf{G}_3(t) + 0.5\zeta_{3Q}^2\mathbf{G}_3^2(t) \\ &\quad + \int_\chi \bigg\{\theta_{3Q}(u)\mathbf{G}_3(t) - \ln\bigg(1+\frac{\theta_{3Q}(u)\mathbf{G}_3(t)}{1+\theta_{3L}(u)}\bigg)\bigg\}\mathfrak{Z}_3^\alpha(\mathrm{d}u). \end{aligned}$$

Then, we obtain

$$\begin{aligned} \mathcal{L}\big(-\ln\mathbf{G}_3(t)\big) &\le -\beta_1\mathcal{H}_1\big(\mathbf{S}_1(t),0\big) - \beta_2\mathcal{H}_2\big(\mathbf{S}_2(t),0\big) + (\mathfrak{u}+\mathfrak{a}+\mathfrak{c}) + 0.5\zeta_{3L}^2 & \text{(A2)} \\ &\quad + \int_\chi \Big(\theta_{3L}(u) - \ln\big(1+\theta_{3L}(u)\big)\Big)\mathfrak{Z}_3^\alpha(\mathrm{d}u) \\ &\quad + \beta_1\Delta_1\big(\mathbf{S}_1(t)-\mathbf{G}_1(t)\big) + \beta_2\Delta_2\big(\mathbf{S}_2(t)-\mathbf{G}_2(t)\big) + \Big(\zeta_{3L}\zeta_{3Q} + \int_\chi \theta_{3Q}(u)\mathfrak{Z}_3^\alpha(\mathrm{d}u)\Big)\mathbf{G}_3(t) \\ &\quad + 0.5\zeta_{3Q}^2\mathbf{G}_3^2(t) + \beta_1\mathcal{H}_1\big(\mathbf{G}_1(t),0\big) - \beta_1\mathcal{H}_1\big(\mathbf{G}_1(t),\mathbf{G}_3(t)\big) & \text{(A3)} \\ &\quad + \beta_2\mathcal{H}_2\big(\mathbf{G}_2(t),0\big) - \beta_2\mathcal{H}_2\big(\mathbf{G}_2(t),\mathbf{G}_3(t)\big). & \text{(A4)} \end{aligned}$$

From systems (2) and (5), we can write

$$
\begin{aligned}
\mathcal{L}\big(\ln \mathbf{S}_1(t)-\ln \mathbf{G}_1(t)\big) \leq & -\frac{\mathfrak{r}}{\mathcal{K}}\big(\mathbf{S}_1(t)-\mathbf{G}_1(t)\big)+\beta_1\mathcal{H}_1\big(\mathbf{G}_1(t),\mathbf{G}_3(t)\big)\frac{\mathbf{G}_3(t)}{\mathbf{G}_1(t)} \\
& -0.5\Big(\big(\zeta_{1L}+\zeta_{1Q}\mathbf{S}_1(t)\big)^2-\big(\zeta_{1L}+\zeta_{1Q}\mathbf{G}_1(t)\big)^2\Big) \\
& +\int_\chi\left\{\ln\left(\frac{1+\theta_{1L}(u)+\theta_{1Q}(u)\mathbf{S}_1(t)}{1+\theta_{1L}(u)+\theta_{1Q}(u)\mathbf{G}_1(t)}\right)-\theta_{1Q}(u)\big(\mathbf{S}_1(t)-\mathbf{G}_1(t)\big)\right\}\mathfrak{Z}_1^\alpha(\mathrm{d}u) \\
\leq & \, \beta_1\Delta_1\mathbf{G}_3(t)-\frac{\mathfrak{r}}{\mathcal{K}}\big(\mathbf{S}_1(t)-\mathbf{G}_1(t)\big) \\
& -\big(\mathbf{S}_1(t)-\mathbf{G}_1(t)\big)\int_\chi\left\{\frac{\theta_{1Q}(u)\big(\theta_{1L}(u)+\theta_{1Q}(u)\mathbf{G}_1(t)\big)}{1+\theta_{1L}(u)+\theta_{1Q}(u)\mathbf{G}_1(t)}\right\}\mathfrak{Z}_1^\alpha(\mathrm{d}u) \\
\leq & \, \beta_1\Delta_1\mathbf{G}_3(t)-\frac{\mathfrak{r}}{\mathcal{K}}\big(\mathbf{S}_1(t)-\mathbf{G}_1(t)\big),
\end{aligned} \tag{A5}
$$

and

$$
\begin{aligned}
\mathcal{L}\big(\ln \mathbf{S}_2(t)-\ln \mathbf{G}_2(t)\big) \leq & \left(\frac{\varpi\mathbf{S}_1(t)}{\mathbf{S}_2(t)}-\frac{\varpi\mathbf{G}_1(t)}{\mathbf{G}_2(t)}\right)+\beta_2\frac{\mathcal{H}_2\big(\mathbf{G}_2(t),\mathbf{G}_3(t)\big)\mathbf{G}_3(t)}{\mathbf{G}_2(t)} \\
& -0.5\Big(\big(\zeta_{2L}+\zeta_{2Q}\mathbf{S}_2(t)\big)^2-\big(\zeta_{2L}+\zeta_{2Q}\mathbf{G}_2(t)\big)^2\Big) \\
& +\int_\chi\left\{\ln\left(\frac{1+\theta_{2L}(u)+\theta_{2Q}(u)\mathbf{S}_2(t)}{1+\theta_{2L}(u)+\theta_{2Q}(u)\mathbf{G}_2(t)}\right)-\theta_{2Q}(u)\big(\mathbf{S}_2(t)-\mathbf{G}_2(t)\big)\right\}\mathfrak{Z}_2^\alpha(\mathrm{d}u) \\
\leq & \, \beta_2\Delta_2\mathbf{G}_3(t)-\zeta_{2L}\zeta_{2Q}\big(\mathbf{S}_2(t)-\mathbf{G}_2(t)\big) \\
& -\big(\mathbf{S}_2(t)-\mathbf{G}_2(t)\big)\int_\chi\left\{\frac{\theta_{2Q}(u)\big(\theta_{2L}(u)+\theta_{2Q}(u)\mathbf{G}_2(t)\big)}{1+\theta_{2L}(u)+\theta_{2Q}(u)\mathbf{G}_2(t)}\right\}\mathfrak{Z}_2^\alpha(\mathrm{d}u) \\
\leq & \, \beta_2\Delta_2\mathbf{G}_3(t)-\zeta_{2L}\zeta_{2Q}\big(\mathbf{S}_2(t)-\mathbf{G}_2(t)\big).
\end{aligned} \tag{A6}
$$

Upon merging relations (A4)–(A6),we have

$$
\begin{aligned}
& \mathcal{L}\bigg(-\ln\mathbf{G}_3(t)+\frac{\Delta_1\beta_1\mathcal{K}}{\mathfrak{r}}\big(\ln\mathbf{S}_1(t)-\ln\mathbf{G}_1(t)\big)+\frac{\Delta_2\beta_2}{\zeta_{2L}\zeta_{2Q}}\big(\ln\mathbf{S}_2(t)-\ln\mathbf{G}_2(t)\big)\bigg) \\
& \leq -\beta_1\mathcal{H}_1\big(\mathbf{S}_1(t),0\big)-\beta_2\mathcal{H}_2\big(\mathbf{S}_2(t),0\big)+(\mathfrak{u}+\mathfrak{a}+\mathfrak{c})+0.5\zeta_{3L}^2 \\
& \quad +\int_\chi\Big(\theta_{3L}(u)-\ln\big(1+\theta_{3L}(u)\big)\Big)\mathfrak{Z}_3^\alpha(\mathrm{d}u) \\
& \quad +\left(\zeta_{3L}\zeta_{3Q}+\int_\chi\theta_{3Q}(u)\mathfrak{Z}_3^\alpha(\mathrm{d}u)\right)\mathbf{G}_3(t)+0.5\zeta_{3Q}^2\mathbf{G}_3^2(t)+\frac{\Delta_1^2\beta_1^2\mathcal{K}}{\mathfrak{r}}\mathbf{G}_3(t) \\
& \quad +\beta_1\mathcal{H}_1\big(\mathbf{G}_1(t),0\big)-\beta_1\mathcal{H}_1\big(\mathbf{G}_1(t),\mathbf{G}_3(t)\big) \\
& \quad +\frac{\Delta_2^2\beta_2^2}{\zeta_{2L}\zeta_{2Q}}\mathbf{G}_3(t)+\beta_2\mathcal{H}_2\big(\mathbf{G}_2(t),0\big)-\beta_2\mathcal{H}_2\big(\mathbf{G}_2(t),\mathbf{G}_3(t)\big) \\
& = -\beta_1\int_{\mathbb{R}_+}\mathcal{H}_1(x,0)\pi^{\mathbf{S}_1}(\mathrm{d}x)-\beta_2\int_{\mathbb{R}_+}\mathcal{H}_2(x,0)\pi^{\mathbf{S}_2}(\mathrm{d}x)+(\mathfrak{u}+\mathfrak{a}+\mathfrak{c})+0.5\zeta_{3L}^2 \\
& \quad +\int_\chi\Big(\theta_{3L}(u)-\ln\big(1+\theta_{3L}(u)\big)\Big)\mathfrak{Z}_3^\alpha(\mathrm{d}u) \\
& \quad +\beta_1\left(\int_{\mathbb{R}_+}\mathcal{H}_1(x,0)\pi^{\mathbf{S}_1}(\mathrm{d}x)-\mathcal{H}_1\big(\mathbf{S}_1(t),0\big)\right)+\beta_2\left(\int_{\mathbb{R}_+}\mathcal{H}_2(x,0)\pi^{\mathbf{S}_2}(\mathrm{d}x)-\mathcal{H}_2\big(\mathbf{S}_2(t),0\big)\right) \\
& \quad +\left(\frac{\Delta_1^2\beta_1^2\mathcal{K}}{\mathfrak{r}}+\frac{\Delta_2^2\beta_2^2}{\zeta_{2L}\zeta_{2Q}}+\zeta_{3L}\zeta_{3Q}+\int_\chi\theta_{3Q}(u)\mathfrak{Z}_3^\alpha(\mathrm{d}u)\right)\mathbf{G}_3(t)+0.5\zeta_{3Q}^2\mathbf{G}_3^2(t) \\
& \quad +\beta_1\mathcal{H}_1\big(\mathbf{G}_1(t),0\big)-\beta_1\mathcal{H}_1\big(\mathbf{G}_1(t),\mathbf{G}_3(t)\big)+\beta_2\mathcal{H}_2\big(\mathbf{G}_2(t),0\big)-\beta_2\mathcal{H}_2\big(\mathbf{G}_2(t),\mathbf{G}_3(t)\big).
\end{aligned}
$$

We select a positive quantity $\phi_\star$ that verifies $\phi_\star \geq \frac{1}{(\mathfrak{u}+\mathfrak{a}+\mathfrak{c})}\left(\frac{\Delta_1^2\beta_1^2\mathcal{K}}{\mathfrak{r}}+\frac{\Delta_2^2\beta_2^2}{\zeta_{2L}\zeta_{2Q}}+\zeta_{3L}\zeta_{3Q}+\int_\chi \theta_{3Q}(u)\mathfrak{Z}_3^\alpha(\mathrm{d}u)\right)$, and we define

$$\mathcal{V}_\star(t) = -\ln \mathbf{G}_3(t) + \frac{\Delta_1\beta_1\mathcal{K}}{\mathfrak{r}}\big(\ln \mathbf{S}_1(t) - \ln \mathbf{G}_1(t)\big) + \frac{\Delta_2\beta_2}{\zeta_{2L}\zeta_{2Q}}\big(\ln \mathbf{S}_2(t) - \ln \mathbf{G}_2(t)\big) + \phi_\star \mathbf{G}_3(t).$$

Then, we have

$$\begin{aligned}
\mathcal{L}\mathcal{V}_\star(t) \leq{}& -\beta_1\int_{\mathbb{R}_+}\mathcal{H}_1(x,0)\pi^{\mathbf{S}_1}(\mathrm{d}x) - \beta_2\int_{\mathbb{R}_+}\mathcal{H}_2(x,0)\pi^{\mathbf{S}_2}(\mathrm{d}x) + (\mathfrak{u}+\mathfrak{a}+\mathfrak{c}) + 0.5\zeta_{3L}^2\\
&+\int_\chi\Big(\theta_{3L}(u) - \ln\big(1+\theta_{3L}(u)\big)\Big)\mathfrak{Z}_3^\alpha(\mathrm{d}u) + \beta_1\bigg(\int_{\mathbb{R}_+}\mathcal{H}_1(x,0)\pi^{\mathbf{S}_1}(\mathrm{d}x) - \mathcal{H}_1(\mathbf{S}_1(t),0)\bigg)\\
&+\beta_2\bigg(\int_{\mathbb{R}_+}\mathcal{H}_2(x,0)\pi^{\mathbf{S}_2}(\mathrm{d}x) - \mathcal{H}_2(\mathbf{S}_2(t),0)\bigg)\\
&+\phi_\star\beta_1\mathcal{H}_1\big(\mathbf{G}_1(t),\mathbf{G}_3(t)\big)\mathbf{G}_3(t) + \phi_\star\beta_2\mathcal{H}_2\big(\mathbf{G}_2(t),\mathbf{G}_3(t)\big)\mathbf{G}_3(t) + 0.5\zeta_{3Q}^2\mathbf{G}_3^2(t)\\
&+\beta_1\mathcal{H}_1\big(\mathbf{G}_1(t),0\big) - \beta_1\mathcal{H}_1\big(\mathbf{G}_1(t),\mathbf{G}_3(t)\big) + \beta_2\mathcal{H}_2\big(\mathbf{G}_2(t),0\big) - \beta_2\mathcal{H}_2\big(\mathbf{G}_2(t),\mathbf{G}_3(t)\big)\\
\leq{}& -\mathfrak{R}_0^\star + \beta_1\bigg(\int_{\mathbb{R}_+}\mathcal{H}_1(x,0)\pi^{\mathbf{S}_1}(\mathrm{d}x) - \mathcal{H}_1(\mathbf{S}_1(t),0)\bigg)\\
&+\beta_2\bigg(\int_{\mathbb{R}_+}\mathcal{H}_2(x,0)\pi^{\mathbf{S}_2}(\mathrm{d}x) - \mathcal{H}_2(\mathbf{S}_2(t),0)\bigg)\\
&+\phi_\star\beta_1\mathcal{H}_1\big(\mathbf{G}_1(t),\mathbf{G}_3(t)\big)\mathbf{G}_3(t) + \phi_\star\beta_2\mathcal{H}_1\big(\mathbf{G}_2(t),\mathbf{G}_3(t)\big)\mathbf{G}_3(t) + 0.5\zeta_{3Q}^2\mathbf{G}_3^2(t)\\
&+\beta_1\mathcal{H}_1\big(\mathbf{G}_1(t),0\big) - \beta_1\mathcal{H}_1\big(\mathbf{G}_1(t),\mathbf{G}_3(t)\big) + \beta_2\mathcal{H}_2\big(\mathbf{G}_2(t),0\big) - \beta_2\mathcal{H}_2\big(\mathbf{G}_2(t),\mathbf{G}_3(t)\big).
\end{aligned}$$

Now, we apply Itô's rule to $(1+\mathbf{G}_1)^p/p$, $(1+\mathbf{G}_2)^p/p$ and $\mathbf{G}_3^p/p$, $\forall 0<p<1$, then

$$\begin{aligned}
\mathcal{L}\bigg(\frac{\mathbf{G}_1^p(t)}{p}\bigg) ={}& \mathbf{G}_1^{p-1}(t)\bigg(\mathfrak{r}\mathbf{G}_1(t)\bigg(1-\frac{\mathbf{G}_1(t)}{\mathcal{K}}\bigg) - \beta_1\mathcal{H}_1\big(\mathbf{G}_1(t),\mathbf{G}_3(t)\big)\mathbf{G}_3(t) - (\mathfrak{u}+\varpi)\mathbf{G}_1(t)\bigg)\\
&+(p-1)0.5\mathbf{G}_1^{p-2}(t)\big(\zeta_{1L}\mathbf{G}_1(t)+\zeta_{1Q}\mathbf{G}_1^2(t)\big)^2\\
&+\int_\chi\bigg\{\frac{\big(\mathbf{G}_1(t)+\theta_{1L}(u)\mathbf{G}_1(t)+\theta_{1Q}(u)\mathbf{G}_1^2(t)\big)^p}{p}\\
&\quad-\frac{\mathbf{G}_1^p(t)}{p} - \mathbf{G}_1^{p-1}(t)\big(\theta_{1L}(u)\mathbf{G}_1(t)+\theta_{1Q}(u)\mathbf{G}_1^2(t)\big)\bigg\}\mathfrak{Z}_1^\alpha(\mathrm{d}u)\\
\leq{}& \mathfrak{r}\mathbf{G}_1^p(t) - 0.5(1-p)\zeta_{1Q}^2\mathbf{G}_1^{p+2}(t),
\end{aligned}$$

$$\begin{aligned}
\mathcal{L}\bigg(\frac{(1+\mathbf{G}_2(t))^p}{p}\bigg) ={}& (1+\mathbf{G}_2(t))^{p-1}\Big(\varpi\mathbf{G}_1(t) - \beta_2\mathcal{H}_2\big(\mathbf{G}_2(t),\mathbf{G}_3(t)\big)\mathbf{G}_3(t) - (\mathfrak{u}+\varsigma)\mathbf{G}_2(t)\Big)\\
&+0.5(p-1)(1+\mathbf{G}_2(t))^{p-2}\big(\zeta_{2L}\mathbf{G}_2(t)+\zeta_{2Q}\mathbf{G}_2^2(t)\big)^2\\
&+\int_\chi\bigg\{\frac{\big((1+\mathbf{G}_2(t))+\theta_{2L}(u)\mathbf{G}_2(t)+\theta_{2Q}(u)\mathbf{G}_2^2(t)\big)^p}{p}\\
&\quad-\frac{(1+\mathbf{G}_2(t))^p}{p} - (1+\mathbf{G}_2(t))^{p-1}\big(\theta_{2L}(u)\mathbf{G}_2(t)+\theta_{2Q}(u)\mathbf{G}_2^2(t)\big)\bigg\}\mathfrak{Z}_2^\alpha(\mathrm{d}u)\\
\leq{}& \varpi\mathbf{G}_1(t) - 0.5(1-p)\zeta_{1Q}^2\mathbf{G}_2^{p+2}(t),
\end{aligned}$$

and

$$\mathcal{L}\left(\frac{\mathbf{G}_3^p(t)}{p}\right) = \mathbf{G}_3^{p-1}(t)\Big(\beta_1\mathcal{H}_1\big(\mathbf{G}_1(t),\mathbf{G}_3(t)\big)\mathbf{G}_3(t) + \beta_2\mathcal{H}_2\big(\mathbf{G}_2(t),\mathbf{G}_3(t)\big)\mathbf{G}_3(t) - (\mathfrak{u}+\mathfrak{a}+\mathfrak{c})\mathbf{G}_3(t)\Big)$$
$$+ 0.5(p-1)\mathbf{G}_3^{p-2}(t)\big(\zeta_{3L}\mathbf{G}_3(t) + \zeta_{3Q}\mathbf{G}_3^2(t)\big)^2$$
$$+ \int_{\mathcal{X}}\Bigg\{\frac{\big(\mathbf{G}_3(t) + \theta_{1L}(u)\mathbf{G}_3(t) + \theta_{1Q}(u)\mathbf{G}_3^2(t)\big)^p}{p}$$
$$- \frac{\mathbf{G}_3^p(t)}{p} - \mathbf{G}_3^p(t)\big(\theta_{3L}(u) + \theta_{3Q}(u)\mathbf{G}_3(t)\big)\Bigg\}\mathfrak{z}_3^{\alpha}(\mathrm{d}u)$$
$$\leq \beta_1\Delta_1\mathbf{G}_1(t)\mathbf{G}_3^p(t) + \beta_2\Delta_2\mathbf{G}_2(t)\mathbf{G}_3^p(t) - \big((\mathfrak{u}+\mathfrak{a}+\mathfrak{c}) + 0.5(1-p)\zeta_{21}^2\big)\mathbf{G}_3^p(t)$$
$$- (1-p)\zeta_{3L}\zeta_{3Q}\mathbf{G}_3^{p+1}(t) - 0.5(1-p)\zeta_{3Q}^2\mathbf{G}_3^{p+2}(t)$$
$$\leq \frac{\beta_1\Delta_1}{p+1}\mathbf{G}_1^{p+1}(t) + \frac{p\beta_1\Delta_1}{p+1}\mathbf{G}_3^{p+1}(t) + \frac{\beta_2\Delta_2}{p+1}\mathbf{G}_2^{p+1}(t) + \frac{p\beta_2\Delta_2}{p+1}\mathbf{G}_3^{p+1}(t) - 0.5(1-p)\zeta_{3Q}^2\mathbf{G}_3^{p+2}(t).$$

Now, we consider the following function

$$\widetilde{\mathcal{V}_\star}\big(\mathbf{G}_1(t),\mathbf{G}_2(t),\mathbf{G}_3(t)\big) = \mathcal{O}_\star\mathcal{V}_\star(t) + \frac{1}{p}\Big\{\mathbf{G}_1^p(t) + \big(1+\mathbf{G}_2(t)\big)^p + \mathbf{G}_3^p(t)\Big\},$$

where $\mathcal{O}_\star > 0$ is a sufficiently large quantity verifying $-\mathcal{O}_\star\mathfrak{R}_0^\star + \mathfrak{G} + 2 \leq 0$, and

$$\mathfrak{G} = \max\Bigg\{\sup_{(\mathbf{G}_1,\mathbf{G}_2,\mathbf{G}_3)\in\mathbb{R}_+^{3,\star}}\Bigg\{\mathfrak{r}\mathbf{G}_1^p - 0.25(1-p)\zeta_{1Q}^2\mathbf{G}_1^{p+2} + \varpi\mathbf{G}_1 - 0.25(1-p)\zeta_{1Q}^2\mathbf{G}_2^{p+2} + \frac{\beta_1\Delta_1}{p+1}\mathbf{G}_1^{p+1}$$
$$+ \frac{p\beta_1\Delta_1}{p+1}\mathbf{G}_3^{p+1} + \frac{\beta_2\Delta_2}{p+1}\mathbf{G}_2^{p+1} + \frac{p\beta_2\Delta_2}{p+1}\mathbf{G}_3^{p+1} - 0.25(1-p)\zeta_{3Q}^2\mathbf{G}_3^{p+2}\Bigg\}, 1\Bigg\}.$$

Since the function $\widetilde{\mathcal{V}_\star}(\mathbf{G}_1,\mathbf{G}_2,\mathbf{G}_3)$ can attains its lower critical bound at a quantity $(\underline{\mathbf{G}_1},\underline{\mathbf{G}_2},\underline{\mathbf{G}_3})$ in $\mathbb{R}_+^3$, we can define the following non-negative Lyapunov function

$$\widetilde{\mathcal{V}_\star}\big(\mathbf{G}_1(t),\mathbf{G}_2(t),\mathbf{G}_3(t)\big) = \mathcal{O}_\star\mathcal{V}_\star(t) + \frac{1}{p}\Big\{\mathbf{G}_1^p(t) + \big(1+\mathbf{G}_2(t)\big)^p + \mathbf{G}_3^p(t)\Big\} - \widetilde{\mathcal{V}_\star}(\underline{\mathbf{G}_1},\underline{\mathbf{G}_2},\underline{\mathbf{G}_3}).$$

So, we get

$$\mathcal{L}\widetilde{\mathcal{V}_\star}\big(\mathbf{G}_1(t),\mathbf{G}_2(t),\mathbf{G}_3(t)\big) \leq -\mathcal{O}_\star\mathfrak{R}_0^\star + \mathcal{O}_\star\beta_1\bigg(\int_{\mathbb{R}_+}\mathcal{H}_1(x,0)\pi^{\mathbf{S}_1}(\mathrm{d}x) - \mathcal{H}_1\big(\mathbf{S}_1(t),0\big)\bigg)$$
$$+ \mathcal{O}_\star\beta_2\bigg(\int_{\mathbb{R}_+}\mathcal{H}_2(x,0)\pi^{\mathbf{S}_2}(\mathrm{d}x) - \mathcal{H}_2\big(\mathbf{S}_2(t),0\big)\bigg)$$
$$+ \mathcal{O}_\star\phi_\star\beta_1\mathcal{H}_1\big(\mathbf{G}_1(t),\mathbf{G}_3(t)\big)\mathbf{G}_3(t) + \mathcal{O}_\star\phi_\star\beta_2\mathcal{H}_2\big(\mathbf{G}_2(t),\mathbf{G}_3(t)\big)\mathbf{G}_3(t) + 0.5\mathcal{O}_\star\zeta_{3Q}^2\mathbf{G}_3^2(t)$$
$$+ \mathcal{O}_\star\beta_1\mathcal{H}_1\big(\mathbf{G}_1(t),0\big) - \mathcal{O}_\star\beta_1\mathcal{H}_1\big(\mathbf{G}_1(t),\mathbf{G}_3(t)\big)$$
$$+ \mathcal{O}_\star\beta_2\mathcal{H}_2\big(\mathbf{G}_2(t),0\big) - \mathcal{O}_\star\beta_2\mathcal{H}_2\big(\mathbf{G}_2(t),\mathbf{G}_3(t)\big)$$
$$+ \mathfrak{r}\mathbf{G}_1^p(t) - 0.5(1-p)\zeta_{1Q}^2\mathbf{G}_1^{p+2}(t) + \varpi\mathbf{G}_1(t) - 0.5(1-p)\zeta_{1Q}^2\mathbf{G}_2^{p+2}(t) + \frac{\beta_1\Delta_1}{p+1}\mathbf{G}_1^{p+1}(t)$$
$$+ \frac{p\beta_1\Delta_1}{p+1}\mathbf{G}_3^{p+1}(t) + \frac{\beta_2\Delta_2}{p+1}\mathbf{G}_2^{p+1}(t) + \frac{p\beta_2\Delta_2}{p+1}\mathbf{G}_3^{p+1}(t) - 0.5(1-p)\zeta_{3Q}^2\mathbf{G}_3^{p+2}(t)$$
$$= f(\mathbf{G}_1,\mathbf{G}_2,\mathbf{G}_3) + \mathcal{O}_\star\beta_1\bigg(\int_{\mathbb{R}_+}\mathcal{H}_1(x,0)\pi^{\mathbf{S}_1}(\mathrm{d}x) - \mathcal{H}_1\big(\mathbf{S}_1(t),0\big)\bigg)$$
$$+ \mathcal{O}_\star\beta_2\bigg(\int_{\mathbb{R}_+}\mathcal{H}_2(x,0)\pi^{\mathbf{S}_2}(\mathrm{d}x) - \mathcal{H}_2\big(\mathbf{S}_2(t),0\big)\bigg).$$

By using the same techniques presented in the demonstration of [Theorem 3.2, [11]], and by the virtue of uniform continuity of the functions $\mathcal{H}_1$ and $\mathcal{H}_2$ (hypothesis $\mathbf{C_b}$), we can easily verify that

$$f(\mathbf{G}_1,\mathbf{G}_2,\mathbf{G}_3) \leq -1, \qquad \forall(\mathbf{G}_1,\mathbf{G}_2,\mathbf{G}_3) \in \mathbb{R}_+^{3,\star} \setminus \mathbb{D}_\epsilon,$$

for a given sufficiently small constant $\epsilon > 0$, where

$$\mathbb{D}_\epsilon = \Big\{(\mathbf{G}_1,\mathbf{G}_2,\mathbf{G}_3) \in \mathbb{R}_+^{3,\star} \,|\; \epsilon \leq \mathbf{G}_1 \leq \epsilon^{-1},\; \epsilon \leq \mathbf{G}_2 \leq \epsilon^{-1},\; \epsilon \leq \mathbf{G}_3 \leq \epsilon^{-1}\Big\}.$$

On the other hand, one can easily show that $\exists\, \varrho_\star > 0$ such that $f(\mathbf{G}_1,\mathbf{G}_2,\mathbf{G}_3) \leq \varrho_\star$, for all $(\mathbf{G}_1,\mathbf{G}_2,\mathbf{G}_3) \in \mathbb{R}_+^{3,\star}$. So, we obtain

$$\begin{aligned}
-\mathbb{E}_{\{\Omega,\mathbb{P}\}}\big(\widetilde{\mathcal{V}_\star}(\mathbf{G}_1(0),\mathbf{G}_2(0),\mathbf{G}_3(0))\big) &\leq \mathbb{E}_{\{\Omega,\mathbb{P}\}}\big(\widetilde{\mathcal{V}_\star}(\mathbf{G}_1(t),\mathbf{G}_2(t),\mathbf{G}_3(t))\big) - \mathbb{E}_{\{\Omega,\mathbb{P}\}}\big(\widetilde{\mathcal{V}_\star}(\mathbf{G}_1(0),\mathbf{G}_2(0),\mathbf{G}_3(0))\big)\\
&= \int_0^t \mathbb{E}_{\{\Omega,\mathbb{P}\}}\big(\mathcal{L}\widetilde{\mathcal{V}_\star}(\mathbf{G}_1(s),\mathbf{G}_2(s),\mathbf{G}_3(s))\big)\mathrm{d}s\\
&\leq \int_0^t \mathbb{E}_{\{\Omega,\mathbb{P}\}}\big(f(\mathbf{G}_1(t),\mathbf{G}_2(t),\mathbf{G}_3(t))\big)\mathrm{d}s\\
&\quad + \mathcal{O}_\star\beta_1\mathbb{E}_{\{\Omega,\mathbb{P}\}}\bigg(\int_0^t\int_{\mathbb{R}_+} \mathcal{H}_1(x,0)\pi^{\mathbf{S}_1}(\mathrm{d}x)\mathrm{d}s - \int_0^t \mathcal{H}_1(\mathbf{S}_1(s),0)\mathrm{d}s\bigg)\\
&\quad + \mathcal{O}_\star\beta_2\mathbb{E}_{\{\Omega,\mathbb{P}\}}\bigg(\int_0^t\int_{\mathbb{R}_+} \mathcal{H}_2(x,0)\pi^{\mathbf{S}_2}(\mathrm{d}x)\mathrm{d}s - \int_0^t \mathcal{H}_2(\mathbf{S}_2(s),0)\mathrm{d}s\bigg).
\end{aligned}$$

By employing the ergodic characteristic of $\mathbf{S}_1(t)$ and $\mathbf{S}_2(t)$, we obtain

$$\begin{aligned}
0 &\leq \liminf_{t\to\infty}\frac{1}{t}\int_0^t \Big(\mathbb{E}_{\{\Omega,\mathbb{P}\}} f(\mathbf{G}_1(t),\mathbf{G}_2(t),\mathbf{G}_3(t))\mathbb{1}_{\{(\mathbf{G}_1(s),\mathbf{G}_2(s),\mathbf{G}_3(s))\in\mathbb{D}_\epsilon^c\}}\\
&\quad + \mathbb{E}_{\{\Omega,\mathbb{P}\}} f(\mathbf{G}_1(s),\mathbf{G}_2(s),\mathbf{G}_3(s))\mathbb{1}_{\{(\mathbf{G}_1(s),\mathbf{G}_2(s),\mathbf{G}_3(s))\in\mathbb{D}_\epsilon\}}\Big)\mathrm{d}s\\
&\leq \liminf_{t\to\infty}\frac{1}{t}\int_0^t \Big(-\mathbb{P}_\Omega\big((\mathbf{G}_1(s),\mathbf{G}_2(s),\mathbf{G}_3(s))\in\mathbb{D}_\epsilon^c\big) + \varrho_\star\mathbb{P}_\Omega\big((\mathbf{G}_1(s),\mathbf{G}_2(s),\mathbf{G}_3(s))\in\mathbb{D}_\epsilon\big)\Big)\mathrm{d}s\\
&= -1 + (1+\varrho_\star)\liminf_{t\to\infty}\frac{1}{t}\int_0^t \mathbb{P}_\Omega\big((\mathbf{G}_1(s),\mathbf{G}_2(s),\mathbf{G}_3(s))\in\mathbb{D}_\epsilon\big)\mathrm{d}s.
\end{aligned}$$

Then

$$\liminf_{t\to\infty}\frac{1}{t}\int_0^t \mathbb{P}_\Omega\big((\mathbf{G}_1(s),\mathbf{G}_2(s),\mathbf{G}_3(s))\in\mathbb{D}_\epsilon\big)\mathrm{d}s \geq \frac{1}{1+\varrho_\star} > 0.$$

That is to say that

$$\liminf_{t\to\infty}\frac{1}{t}\int_0^t \mathbb{P}_\Omega\big((\mathbf{G}_1(0),\mathbf{G}_2(0),\mathbf{G}_3(0));s,\mathbb{D}_\epsilon\big)\mathrm{d}s \geq \frac{1}{1+\varrho_\star} > 0, \quad \forall(\mathbf{G}_1(0),\mathbf{G}_2(0),\mathbf{G}_3(0)) \in \mathbb{R}_+^{3,\star}.$$

In accordance with Lemma 5, the demonstration of Theorem 1 is finished.

Appendix C. Proof of Theorem 2

This proof is divided into two parts.
Part I. By using the Itô's formula, we get

$$\begin{aligned}
\mathrm{d}\ln\mathbf{G}_3(t) &= \Big(\beta_1\mathcal{H}_1(\mathbf{G}_1(t),\mathbf{G}_3(t)) + \beta_2\mathcal{H}_2(\mathbf{G}_2(t),\mathbf{G}_3(t)) - (\mathfrak{u}+\mathfrak{a}+\mathfrak{c}) - 0.5\big(\zeta_{3L}+\zeta_{3Q}\mathbf{G}_3(t)\big)^2\\
&\quad + \int_\chi \Big(\ln\big(1+\theta_{3L}(u)+\theta_{3Q}(u)\mathbf{G}_3(t)\big) - \big(\theta_{3L}(u)+\theta_{3Q}(u)\mathbf{G}_3(t)\big)\Big)\mathfrak{Z}_3^\alpha(\mathrm{d}u)\Big)\mathrm{d}t\\
&\quad + (\zeta_{3L}+\zeta_{3Q}\mathbf{G}_3(t))\mathrm{d}\mathcal{B}_3(t) + \int_\chi \ln\big(1+\theta_{3L}(u)+\theta_{3Q}(u)\mathbf{G}_3(t^-)\big)\widetilde{\mathcal{C}}_3^\alpha(\mathrm{d}t,\mathrm{d}u).
\end{aligned}$$

From Lemma 3, we obtain

$$
\begin{aligned}
\mathrm{d}\ln \mathbf{G}_3(t) \leq \Big(& \beta_1 \mathcal{H}_1\big(\mathbf{S}_1(t),0\big) + \beta_2 \mathcal{H}_2\big(\mathbf{S}_2(t),0\big) - (\mathfrak{u}+\mathfrak{a}+\mathfrak{c}) - 0.5\big(\zeta_{3L} + \zeta_{3Q}\mathbf{G}_3(t)\big)^2 \\
& + \int_{\chi} \Big(\ln\big(1+\theta_{3L}(u)+\theta_{3Q}(u)\mathbf{G}_3(t)\big) - \big(\theta_{3L}(u)+\theta_{3Q}(u)\mathbf{G}_3(t)\big)\Big)\mathfrak{Z}_3^{\alpha}(\mathrm{d}u)\Big)\mathrm{d}t \\
& + \big(\zeta_{3L} + \zeta_{3Q}\mathbf{G}_3(t)\big)\mathrm{d}\mathcal{B}_3(t) + \int_{\chi} \ln\big(1+\theta_{3L}(u)+\theta_{3Q}(u)\mathbf{G}_3(t^-)\big)\widetilde{\mathcal{C}}_3^{\alpha}(\mathrm{d}t,\mathrm{d}u).
\end{aligned}
$$

Upon integrating the preceding inequality and dividing both sides by t, yields

$$
\begin{aligned}
\frac{\ln \mathbf{G}_3(t) - \ln \mathbf{G}_3(0)}{t} \leq & \frac{\beta_1}{t}\int_0^t \mathcal{H}_1\big(\mathbf{S}_1(s),0\big)\mathrm{d}s + \frac{\beta_2}{t}\int_0^t \mathcal{H}_2\big(\mathbf{S}_2(s),0\big)\mathrm{d}s - (\mathfrak{u}+\mathfrak{a}+\mathfrak{c}) - 0.5\zeta_{3L}^2 \\
& - \int_{\chi}\Big(\theta_{3L}(u) - \ln\big(1+\theta_{3L}(u)\big)\Big)\mathfrak{Z}_3^{\alpha}(\mathrm{d}u) - \frac{\zeta_{3L}\zeta_{3Q}}{t}\int_0^t \mathbf{G}_3(s)\mathrm{d}s \\
& - \frac{0.5\zeta_{3Q}^2}{t}\int_0^t \mathbf{G}_3^2(s)\mathrm{d}s + \frac{1}{t}\int_0^t \zeta_{3L}\mathrm{d}\mathcal{B}_3(s) \\
& + \frac{1}{t}\int_0^t\int_{\chi}\left[\ln\left(1+\frac{\theta_{3Q}(u)\mathbf{G}_3(s)}{1+\theta_{3L}(u)}\right) - \theta_{3Q}(u)\mathbf{G}_3(s)\right]\mathfrak{Z}_3^{\alpha}(\mathrm{d}u)\mathrm{d}s \\
& + \frac{1}{t}\int_0^t \zeta_{3Q}\mathbf{G}_3(s)\mathrm{d}\mathcal{B}_3(s) + \frac{1}{t}\int_0^t\int_{\chi}\ln\big(1+\theta_{3L}(u)\big)\widetilde{\mathcal{C}}_3^{\alpha}(\mathrm{d}s,\mathrm{d}u) \\
& + \frac{1}{t}\int_0^t\int_{\chi}\ln\left(1+\frac{\theta_{3Q}(u)\mathbf{G}_3(s^-)}{1+\theta_{3L}(u)}\right)\widetilde{\mathcal{C}}_3^{\alpha}(\mathrm{d}s,\mathrm{d}u).
\end{aligned}
$$

We let

$$
\begin{cases}
\mathcal{Z}_1(t) = \displaystyle\int_0^t \zeta_{3L}\mathrm{d}\mathcal{B}_3(s), \\
\mathcal{Z}_2(t) = \displaystyle\int_0^t\int_{\chi}\ln\big(1+\theta_{3L}(u)\big)\widetilde{\mathcal{C}}_3^{\alpha}(\mathrm{d}s,\mathrm{d}u).
\end{cases}
$$

It is so simple to check that their quadratic variants are determined by

$$
\begin{cases}
\langle \mathcal{Z}_1(t), \mathcal{Z}_1(t)\rangle = \zeta_{3L}^2 t, \\
\langle \mathcal{Z}_2(t), \mathcal{Z}_2(t)\rangle = t\displaystyle\int_{\chi}\Big(\ln\big(1+\theta_{3L}(u)\big)\Big)^2\mathfrak{Z}_3^{\alpha}(\mathrm{d}u).
\end{cases}
$$

Consequently, we obtain as $t \to \infty$,

$$
\begin{cases}
t^{-1}\ \mathcal{Z}_1(t) \to 0 \ \text{ a.s.} \\
t^{-1}\ \mathcal{Z}_2(t) \to 0 \ \text{ a.s.}
\end{cases}
$$

In line with the exponential inequality for martingales, we get

$$
\begin{aligned}
\mathbb{P}_{\Omega}\Bigg\{ \sup_{0\leq t\leq \mathfrak{n}_{\star}} \Bigg[& \int_0^t \zeta_{3Q}\mathbf{G}_3(s)\mathrm{d}\mathcal{B}_3(s) - 0.5\int_0^t \zeta_{3Q}^2\mathbf{G}_3^2(s)\mathrm{d}s \\
& - \int_0^t\int_{\chi}\left(\left(\frac{\theta_{3Q}(u)\mathbf{G}_3(s)}{1+\theta_{3L}(u)}\right) + \ln\left(1+\frac{\theta_{3Q}(u)\mathbf{G}_3(s)}{1+\theta_{3L}(u)}\right)\right)\mathfrak{Z}_3^{\alpha}(\mathrm{d}u)\mathrm{d}s \\
& + \int_0^t\int_{\chi}\ln\left(1+\frac{\theta_{3Q}(u)\mathbf{G}_3(s^-)}{1+\theta_{3L}(u)}\right)\widetilde{\mathcal{C}}_3^{\alpha}(\mathrm{d}s,\mathrm{d}u)\Bigg] \geq 2\ln\mathfrak{n}_{\star}\Bigg\} \leq \frac{1}{\mathfrak{n}_{\star}^2}.
\end{aligned}
$$

Borel-Cantelli Lemma stated that for almost $\omega \in \Omega$, we have the existence of an integer $\mathfrak{n}_{\star,\omega} > 0$ such that for all $n \geq \mathfrak{n}_{\star,\omega}$, $t \in [\mathfrak{n}_\star - 1, \mathfrak{n}_\star) \subseteq \mathbb{R}_+$ a.s.,

$$2\ln\mathfrak{n}_\star + 0.5\int_0^t \zeta_{3Q}^2\mathbf{G}_3^2(s)\mathrm{d}s + \int_0^t\int_\chi \left(\left(\frac{\theta_{3Q}(u)\mathbf{G}_3(s)}{1+\theta_{3L}(u)}\right) - \ln\left(1+\frac{\theta_{3Q}(u)\mathbf{G}_3(s)}{1+\theta_{3L}(u)}\right)\right)\mathfrak{Z}_3^\alpha(\mathrm{d}u)\mathrm{d}s$$
$$\geq \int_0^t \zeta_{3Q}\mathbf{G}_3(s)\mathrm{d}\mathcal{B}_3(s) + \int_0^t\int_\chi \ln\left(1+\frac{\theta_{3Q}(u)\mathbf{G}_3(s^-)}{1+\theta_{3L}(u)}\right)\widetilde{\mathcal{C}}_3^\alpha(\mathrm{d}s,\mathrm{d}u).$$

So, for every $\mathfrak{n}_\star \geq \mathfrak{n}_{\star,\omega}$ and t in $[-1+\mathfrak{n}_\star, \mathfrak{n}_\star)$ a.s., we have

$$\begin{aligned}\frac{\ln\mathbf{G}_3(t) - \ln\mathbf{G}_3(0)}{t} \leq & \left[\frac{\beta_1}{t}\int_0^t \mathcal{H}_1(\mathbf{S}_1(s),0)\mathrm{d}s + \frac{\beta_2}{t}\int_0^t \mathcal{H}_2(\mathbf{S}_2(s),0)\mathrm{d}s - (\mathfrak{u}+\mathfrak{a}+\mathfrak{c}) - 0.5\zeta_{3L}^2\right.\\ & \left. - \int_\chi\left(\theta_{3L}(u) - \ln(1+\theta_{3L}(u))\right)\mathfrak{Z}_3^\alpha(\mathrm{d}u)\right] - \frac{\zeta_{3L}\zeta_{3Q}}{t}\int_0^t \mathbf{G}_3(s)\mathrm{d}s\\ & + \frac{1}{t}\int_0^t\int_\chi\left(\left(\frac{\theta_{3Q}(u)\mathbf{G}_3(s)}{1+\theta_{3L}(u)}\right) - \theta_{3Q}(u)\mathbf{G}_3(s)\right)\mathfrak{Z}_3^\alpha(\mathrm{d}u)\mathrm{d}s\\ & + \frac{\mathcal{Z}_1(t)}{t} + \frac{\mathcal{Z}_2(t)}{t} + \frac{2\ln\mathfrak{n}_\star}{\mathfrak{n}_\star - 1}.\end{aligned}$$

We take the superior limit on both sides of the last result and obtained the following

$$\begin{aligned}\limsup_{t\to\infty}\frac{\ln\mathbf{G}_3(t)}{t} \leq & \beta_1\int_{\mathbb{R}_+}\mathcal{H}_1(x,0)\pi^{\mathbf{S}_1}(\mathrm{d}x) + \beta_2\int_{\mathbb{R}_+}\mathcal{H}_2(x,0)\pi^{\mathbf{S}_2}(\mathrm{d}x) - (\mathfrak{u}+\mathfrak{a}+\mathfrak{c})\\ & - 0.5\zeta_{3L}^2 - \int_\chi\left(\theta_{3L}(u) - \ln(1+\theta_{3L}(u))\right)\mathfrak{Z}_3^\alpha(\mathrm{d}u)\\ = & \mathfrak{R}_0^\star < 0.\end{aligned}$$

Since the exponential extinction implies the stochastic extinction [50], so $\lim_{t\to\infty}\mathbf{G}_3(t) = 0$ a.s. and the infection of (2) will go to extinction with probability one.
Part II. Based on the result of Part I, we can conclude that for a small $\mathfrak{r}_\star > 0$, we have the existence of $\mathfrak{t}_0$ and $\Omega_{\mathfrak{r}_\star} \subset \Omega$ such that $\mathbb{P}_\Omega(\Omega_{\mathfrak{r}_\star}) > 1 - \mathfrak{r}_\star$ and

$$\begin{cases}\mathcal{H}_1(\mathbf{G}_1,\mathbf{G}_3)\mathbf{G}_3 \leq \mathcal{H}_1(\mathbf{G}_1,0)\mathbf{G}_3 \leq \Delta_1\mathfrak{r}_\star\mathbf{G}_1,\\ \mathcal{H}_2(\mathbf{G}_2,\mathbf{G}_3)\mathbf{G}_3 \leq \mathcal{H}_2(\mathbf{G}_2,0)\mathbf{G}_3 \leq \Delta_2\mathfrak{r}_\star\mathbf{G}_2.\end{cases}$$

Thus

$$\begin{aligned}&\left(\mathfrak{r}\mathbf{G}_1(t)\left(1-\frac{\mathbf{G}_1(t)}{\mathcal{K}}\right) - \beta_1\Delta_1\mathfrak{r}_\star\mathbf{G}_1 - (\mathfrak{u}+\varpi)\mathbf{G}_1(t)\right)\mathrm{d}t + \mathrm{d}\mathbf{S}_1(t)\\ &\leq \mathrm{d}\mathbf{G}_1(t)\\ &\leq \left(\mathfrak{r}\mathbf{G}_1(t)\left(1-\frac{\mathbf{G}_1(t)}{\mathcal{K}}\right) - (\mathfrak{u}+\varpi)\mathbf{G}_1(t)\right)\mathrm{d}t + \mathrm{d}\mathbf{S}_1(t),\end{aligned}$$

and

$$\left(\varpi\mathbf{G}_1(t) - \beta_2\Delta_2\mathfrak{r}_\star\mathbf{G}_2 - (\mathfrak{u}+\varsigma)\mathbf{G}_2(t)\right)\mathrm{d}t + \mathrm{d}\mathbf{S}_2(t) \leq \mathrm{d}\mathbf{G}_2(t) \leq (\varpi\mathbf{G}_1(t) - \mathfrak{u}\mathbf{G}_2(t))\mathrm{d}t + \mathrm{d}\mathbf{S}_2(t),$$

indicating that the distributions of $\mathbf{S}_1(t)$ and $\mathbf{S}_2(t)$ converge weakly to $\pi^{\mathbf{S}_1}(\cdot)$ and $\pi^{\mathbf{S}_2}(\cdot)$, respectively. The demonstration is finished.

References

1. Hays, J.N. *Epidemics and Pandemics: Their Impacts on Human History*; Abc-Clio: Santa Barbara, CA, USA, 2005.
2. Ministry of Health of Morocco. Available online: www.sante.gov.ma (accessed on 15 November 2022).
3. May, R.M. *Stability and Complexity in Model Ecosystems*; Princeton Landmarks in Biology; Princeton University Press: Princeton, NJ, USA, 2001.

4. Nair, S. *Advanced Topics in Applied Mathematics: For Engineering and the Physical Sciences*; Cambridge University Press: Cambridge, UK, 2011.
5. Kermack, W.O.; McKendrick, A.G. A contribution to the mathematical theory of epidemics. *Proc. R. Soc. Math. Phys. Eng. Sci.* **1927**, *115*, 700–721.
6. Heymann, D.L.; Shindo, N. COVID-19: What is next for public health? *Lancet* **2020**, *395*, 542–545. [CrossRef] [PubMed]
7. Buonomo, B. Effects of information-dependent vaccination behavior on coronavirus outbreak: Insights from a SIRI model. *Ric. Mat.* **2020**, *69*, 483–499. [CrossRef]
8. Harianto, J.; Sari, I.P. Local Dynamics of an SVIR Epidemic Model with Logistic Growth. *Cauchy—J. Mat. Murni Dan Apl.* **2020**, *6*, 122–132. [CrossRef]
9. Horsthemke, W.; Lefever, R. *Noise-Induced Transitions: Theory and Applications in Physics, Chemistry, and Biology*; Springer: Berlin/Heidelberg, Germany, 1984.
10. Sabbar, Y.; Yavuz, M.; Ozkose, F. Infection Eradication Criterion in a General Epidemic Model with Logistic Growth, Quarantine Strategy, Media Intrusion, and Quadratic Perturbation. *Mathematics* **2022**, *10*, 4213. [CrossRef]
11. Sabbar, Y.; Kiouach, D.; Rajasekar, S.P.; El-Idrissi, S.E.A. The influence of quadratic Lévy noise on the dynamic of an SIC contagious illness model: New framework, critical comparison and an application to COVID-19 (SARS-CoV-2) case. *Chaos Solitons Fractals* **2022**, *159*, 112110. [CrossRef]
12. Din, A.; Khan, A.; Sabbar, Y. Long-Term Bifurcation and Stochastic Optimal Control of a Triple-Delayed Ebola Virus Model with Vaccination and Quarantine Strategies. *Fractal Fract.* **2022**, *6*, 578. [CrossRef]
13. Khan, A.; Sabbar, Y.; Din, A. Stochastic modeling of the Monkeypox 2022 epidemic with cross-infection hypothesis in a highly disturbed environment. *Math. Biosci. Eng. MBE* **2022**, *19*, 13560–13581. [CrossRef]
14. Ciuchi, S.; Pasquale, F.D.; Spagnolo, B. Nonlinear relaxation in the presence of an absorbing barrier. *Phys. Rev. E* **1993**, *47*, 3915. [CrossRef]
15. Din, A.; Khan, A.; Baleanu, D. Stationary distribution and extinction of stochastic coronavirus (COVID-19) epidemic model. *Chaos Solitons Fractals* **2020**, *139*, 110036. [CrossRef]
16. Din, A.; Li, Y.; Khan, T.; Zaman, G. Mathematical analysis of spread and control of the novel corona virus (COVID-19) in China. *Chaos Solitons Fractals* **2020**, *141*, 110286. [CrossRef]
17. Din, A.; Li, Y.; Yusuf, A. Delayed hepatitis B epidemic model with stochastic analysis. *Chaos Solitons Fractals* **2020**, *146*, 110839. [CrossRef]
18. Spagnolo, B.; Cirone, M.; Barbera, A.L.; Pasquale, F.D. Noise-induced effects in population dynamics. *J. Physics Condens. Matter* **2002**, *14*, 2247. [CrossRef]
19. Zhao, Y.; Jiang, D. The behavior of an SVIR epidemic model with stochastic perturbation. *Abstr. Appl. Anal.* **2014**, *2014*. [CrossRef]
20. Zhang, X.; Yang, Q. Threshold behavior in a stochastic SVIR model with general incidence rates. *Appl. Math. Lett.* **2021**, *121*, 107403. [CrossRef]
21. Dieu, N.T.; Nguyen, D.H.; Du, N.H.; Yin, G. Classification of asymptotic behavior in a stochastic SIR model. *SIAM J. Appl. Dyn. Syst.* **2016**, *15*, 1062–1084. [CrossRef]
22. Liu, Q.; Jiang, D.; Hayat, T.; Ahmed, B. Periodic solution and stationary distribution of stochastic SIR epidemic models with higher order perturbation. *Phys. A* **2017**, *482*, 209–217. [CrossRef]
23. Liu, Q.; Jiang, D. Stationary distribution and extinction of a stochastic SIR model with nonlinear perturbation. *Appl. Math. Lett.* **2017**, *73*, 8–15. [CrossRef]
24. Liu, Q.; Jiang, D.; Hayat, T.; Ahmed, B. Stationary distribution and extinction of a stochastic predator-prey model with additional food and nonlinear perturbation. *Appl. Math. Comput.* **2018**, *320*, 226–239. [CrossRef]
25. Lv, X.; Meng, X.; Wang, X. Extinction and stationary distribution of an impulsive stochastic chemostat model with nonlinear perturbation. *Chaos Solitons Fractals* **2018**, *110*, 273–279. [CrossRef]
26. Dieu, N.T.; Fugo, T.; Du, N.H. Asymptotic behaviors of stochastic epidemic models with jump-diffusion. *Appl. Math. Model.* **2020**, *86*, 259–270. [CrossRef]
27. Kiouach, D.; Sabbar, Y. Developing new techniques for obtaining the threshold of a stochastic SIR epidemic model with 3-dimensional Levy process. *J. Appl. Nonlinear Dyn.* **2022**, *11*, 401–414. [CrossRef]
28. Kiouach, D.; Sabbar, Y. The long-time behaviour of a stochastic SIR epidemic model with distributed delay and multidimensional Levy jumps. *Int. J. Biomath.* **2021**, *2021*, 2250004.
29. Rosinski, J. Tempering stable processes. *Stoch. Process. Their Appl.* **2007**, *117*, 677–707. [CrossRef]
30. Guo, B.; Khan, A.; Din, A. Numerical Simulation of Nonlinear Stochastic Analysis for Measles Transmission: A Case Study of a Measles Epidemic in Pakistan. *Chaos Solitons Fractals* **2023**, *7*, 130. [CrossRef]
31. Kiouach, D.; Sabbar, Y. Stability and Threshold of a Stochastic SIRS Epidemic Model with Vertical Transmission and Transfer from Infectious to Susceptible Individuals. *Discret. Dyn. Nat. Soc.* **2018**, *2018*, 7570296. [CrossRef]
32. Kiouach, D.; Sabbar, Y.; El-idrissi, S.E.A. New results on the asymptotic behavior of an SIS epidemiological model with quarantine strategy, stochastic transmission, and Levy disturbance. *Math. Methods Appl. Sci.* **2021**, *44*, 13468–13492. [CrossRef]
33. Kiouach, D.; Sabbar, Y. Dynamic characterization of a stochastic SIR infectious disease model with dual perturbation. *Int. J. Biomath.* **2021**, *14*, 2150016. [CrossRef]

34. Kiouach, D.; Sabbar, Y. Ergodic Stationary Distribution of a Stochastic Hepatitis B Epidemic Model with Interval-Valued Parameters and Compensated Poisson Process. *Comput. Math. Methods Med.* **2020**, *2020*, 9676501. [CrossRef]
35. Kiouach, D.; Sabbar, Y. The threshold of a stochastic SIQR epidemic model with Levy jumps. *Trends Biomath. Math. Model. Health Harvest. Popul. Dyn.* **2019**, *2019*, 87–105.
36. Levy, S. Wealthy people and fat tails: An explanation for the Lévy distribution of stock returns. *UCLA Financ.* **1998**, *1998*. Available online: https://escholarship.org/uc/item/5zf0f3tg (accessed on 15 November 2022).
37. Levy, M. Market efficiency, the Pareto wealth distribution, and the Levy distribution of stock returns. *Econ. Evol. Complex Syst. III Curr. Perspect. Future Dir.* **2005**, *2005*, 101–132.
38. Sabbar, Y.; Khan, A.; Din, A. Probabilistic analysis of a marine ecological system with intense variability. *Mathematics* **2022**, *10*, 2262. [CrossRef]
39. Sabbar, Y.; Khan, A.; Din, A.; Kiouach, D.; Rajasekar, S.P. Determining the global threshold of an epidemic model with general interference function and high-order perturbation. *AIMS Math.* **2022**, *7*, 19865–19890. [CrossRef]
40. Naim, M.; Abbar, S.Y.; Zeb, A. Stability characterization of a fractional-order viral system with the non-cytolytic immune assumption. *Math. Model. Numer. Simul. Appl.* **2022**, *2*, 164–176. [CrossRef]
41. Sabbar, Y.; Zeb, A.; Gul, N.; Kiouach, D.; Rajasekar, S.P.; Ullah, N.; Mohammad, A. Stationary distribution of an SIR epidemic model with three correlated Brownian motions and general Lévy measure. *AIMS Math.* **2023**, *8*, 1329–1344. [CrossRef]
42. Sabbar, Y.; Kiouach, D.; Rajasekar, S.P. Acute threshold dynamics of an epidemic system with quarantine strategy driven by correlated white noises and Lévy jumps associated with infinite measure. *Int. J. Dyn. Control.* **2022**, *2022*, 1–14. [CrossRef]
43. Zhou, Y.; Zhang, W.; Yuan, S. Survival and stationary distribution of a SIR epidemic model with stochastic perturbations. *Appl. Math. Comput.* **2014**, *244*, 118–131. [CrossRef]
44. Lv, J.; Liu, H.; Zou, X. Stationary distribution and persistence of a stochastic predator-prey model with a functional response. *J. Appl. Anal. Comput.* **2019**, *9*, 1–11. [CrossRef]
45. Zhao, Y.; Jiang, D. The threshold of a stochastic SIS epidemic model with vaccination. *Appl. Math. Comput.* **2014**, *243*, 718–727. [CrossRef]
46. Peng, S.; Zhu, X. Necessary and sufficient condition for comparison theorem of 1-dimensional stochastic differential equations. *Stoch. Process. Their Appl.* **2006**, *116*, 370–380. [CrossRef]
47. Stettner, L. On the existence and uniqueness of invariant measure for continuous-time Markov processes. *Tech. Rep. Lcds Brown Univ. Prov.* **1986**, 18–86.
48. Privault, N.; Wang, L. Stochastic SIR Levy Jump Model with Heavy Tailed Increments. *J. Nonlinear Sci.* **2021**, *31*, 1–28. [CrossRef]
49. Xi, F. Asymptotic properties of jump-diffusion processes with state-dependent switching. *Stoch. Process. Their Appl.* **2009**, *119*, 2198–2221. [CrossRef]
50. Mao, X. *Stochastic Differential Equations and Applications*; Elsevier: Amsterdam, The Netherlands, 2007.
51. Tong, J.; Zhang, Z.; Bao, J. The stationary distribution of the facultative population model with a degenerate noise. *Stat. Probab. Lett.* **2013**, *83*, 655–664. [CrossRef]